Worcester Polytechnic Institute
Digital WPI

Major Qualifying Projects (All Years) | Major Qualifying Projects

April 2015

Automated System for High-throughput Chemical Screening in C. elegans

Benjamin Minich Altshuler
Worcester Polytechnic Institute

Michelle Joann Zayas
Worcester Polytechnic Institute

Sneha Priya Shastry
Worcester Polytechnic Institute

Thomas Brian Biernacki
Worcester Polytechnic Institute

Follow this and additional works at: https://digitalcommons.wpi.edu/mqp-all

Repository Citation
Altshuler, B. M., Zayas, M. J., Shastry, S. P., & Biernacki, T. B. (2015). *Automated System for High-throughput Chemical Screening in C. elegans*. Retrieved from https://digitalcommons.wpi.edu/mqp-all/870

This Unrestricted is brought to you for free and open access by the Major Qualifying Projects at Digital WPI. It has been accepted for inclusion in Major Qualifying Projects (All Years) by an authorized administrator of Digital WPI. For more information, please contact digitalwpi@wpi.edu.

Automated system for high-throughput chemical screening in *C. elegans*

A Major Qualifying Project Report:

Submitted to the Faculty

Of the

WORCESTER POLYTECHNIC INSTITUTE

In partial fulfillment of the requirements for the

Degree of Bachelor of Science

by

Benjamin Altshuler

Thomas Biernacki

Sneha Shastry

Michelle Zayas

Date: April 30, 2015

Approved:

Prof. Dirk R. Albrecht, Major Advisor

1. *C. elegans*
2. High-throughput
3. Automated chemical screening

Table of Contents

Table of Authorship

Chapter 1: Introduction – All
Chapter 2: Literature Review – SS
- 2.1 Neuroscience – SS
  - 2.1.1 Neurobiology – BA
  - 2.1.2 Neuropsychiatric Disorders – SS
  - 2.1.3 Drug Research – SS
- 2.2 *C. elegans* – BA
  - 2.2.1 History of *C. elegans* Research – MZ
  - 2.2.2 *C. elegans* Anatomy – MZ
  - 2.2.3 Genetics – TB
  - 2.2.4 Research Applications – MZ
- 2.3 Chemical Screening – SS
  - 2.3.1 Manual Process of Chemical Screening – BA
  - 2.3.2 Automated Systems – TB
  - 2.3.3 Arduino System – SS

Chapter 3: Project Strategy – BA
- 3.1 Client Statement – BA, SS, MZ
- 3.2 Objectives – TB, SS
  - 3.2.1 Accurate – BA
  - 3.2.2 Precise – SS, MZ
  - 3.2.3 Efficient – SS, MZ
  - 3.2.4 Safe – TB, SS, BA
  - 3.2.5 User Friendly – TB, BA
- 3.3 Constraints – SS
- 3.4 Project Approach – SS

Chapter 4: Design Alternatives – SS
- 4.1 Needs Analysis – SS
- 4.2 Conceptual Designs – TB, SS
- 4.3 Functions (Specifications) – SS, BA
- 4.4 Preliminary/Alternative Designs – TB, MZ
- 4.5 Feasibility Study/Experiments – TB, BA
- 4.6 Modeling – MZ
- 4.7 Preliminary Data
  - 4.7.1 Load Test from SolidWorks – MZ
  - 4.7.2 Arduino and Slide Potentiometer – SS
  - 4.7.3 Z-Axis Mounting – TB
  - 4.7.4 Initial Dye Test – BA

Chapter 5: Design Verification & Results – SS, BA
- 5.1 Chemical Switching Rate – SS, MZ, BA
- 5.2 Cross-Contamination Study – MZ, BA
- 5.3 *C. elegans* Automated Chemical Screen – BA

Chapter 6: Discussion – SS
Chapter 7: Final Design – TB
Chapter 8: Conclusion and Recommendations – SS, TB

Table of Figures

Table of Tables

Acknowledgements

We would like to thank our advisor, Dirk Albrecht, PhD, for all of his guidance, help, and encouragement throughout the year. We would also like to thank Ross Lagoy for his assistance in setting up experiments and analyzing and interpreting our data. Additionally, we appreciate the help of Lisa Wall, Professor Raymond Page, Professor Zoe Reidinger, Laura Aurilio, and Kyra Burnett throughout the course of our project.

Abstract

Neuropsychiatric disorders alter neural activity in those who suffer from these diseases. High-throughput screening can be used to find drugs with fewer debilitating side effects than current treatments. *C. elegans* nematodes are ideal models for high-throughput testing and for observing neural activity in intact neural circuits, but current screening experiments using *C. elegans* are conducted manually, which is time-consuming and hands-on for the researcher. Automated screening systems save time and effort, but are expensive and cannot be tailored to fit the specific needs of neural imaging in *C. elegans*. We designed an automated, modular, and inexpensive system for use in chemical screening with *C. elegans*. This improved chemical delivery system used off-the-shelf robotic hardware, a 3D-printed microplate tray, and open-source electronics and control software, costing ~$300. Our method sequentially delivers test chemicals from a 96-well microplate, with low cross-contamination (<0.01%) and satisfactory switching speed (<1 min) between chemicals. We validated our system by reproducing the dose-response results published in a previous *C. elegans* chemical screening experiment.

Keywords—C. elegans, automation, high-throughput screening, neural imaging

Chapter 1: Introduction

The brain is the least understood organ in the human body. Responsible for a wide variety of functions, the brain allows us to think, remember, perceive, control movements, and interact with one another. Approximately 86 billion neurons, or nervous system cells, communicate to relay and process information throughout the body via electrical and chemical signals (Azevedo et al. 2009). The health of these cells and their connections is imperative to the execution of neurological functions. Unfortunately, neurological disorders can hinder these processes due to malfunctions in the nervous system, causing decreased functionality in behavior and cognition. In diseases like schizophrenia and autism, the complex factors that cause these functional deficits are relatively unknown.

Schizophrenia and autism are two prevalent neuropsychiatric disorders that adversely affect patients' quality of life. While these conditions can be managed with medicinal and psychiatric interventions, neither of them is curable. Furthermore, the drugs that are used to alleviate symptoms, most commonly antipsychotic drugs, often result in adverse side effects, one of which is the increased risk of venous thromboembolism (Parker et al. 2010). Due to the immense complexity of mammalian neural systems, these disorders are difficult to study in such models, especially in human beings. For this reason, as well as many others, *Caenorhabditis elegans* (*C. elegans*) is a promising model system for *in vivo* neuropsychiatric disorder research and drug discovery.

Researchers have explored various animal models to test novel neurotherapeutics with the end-goal of finding a treatment for neurological diseases. Conducting experiments using mammalian models, such as rodents, is marked by challenges. In a neuroprotective therapy study, approximately 500 drugs were tested on rodent models, but only one of these drugs passed

clinical trials and became an approved therapy (Chesselet, 2012). This example emphasizes the degree of throughput needed to adequately screen for drug options. Additionally, due to the large library of drugs that remain to be tested for the treatment of neurological diseases, mammalian systems are not practical models. Microscopic nematodes are a viable alternative, providing a number of benefits, one being their capacity for high-throughput applications. *C. elegans*, which are microscopic, transparent roundworms (approximately 1 mm long), are an ideal animal model for a number of reasons. They are easy to maintain, since they require a simple environment (agar filled petri dish) and food source (*E. coli*) for growth, and they reach maturity in three days, allowing for convenient experiment staging. The nematode's transparent body provides a clear visualization of internal structures and processes. *C. elegans* contain exactly 959 cells, 302 of which are neurons and 95 of which are body wall muscles. *C. elegans* was the first animal to have its genome fully sequenced, with further studies resulting in the complete mapping of its neural network (Sleigh, 2010). *C. elegans* genes are also 50 percent homologous to human genes, and their proteomes are 83 percent homologous to those of humans, making them suitable models for neuropsychiatric disease research (Caldwell, 2008; Lai et al, 2000). Scientists can manipulate and mutate *C. elegans* to match the same diseased genes that would be present in human patients, thus increasing their utility as neuropsychiatric models. Testing many different therapies for neurological diseases on mutated worms, high-throughput chemical screening involves sequentially introducing chemicals or chemical cocktails to a microfluidic arena where the *C. elegans* reside. Upon exposure to the stimuli, the worms typically respond, and these responses can be quantified behaviorally and neurologically using computer software (MATLAB, ImageJ, etc.) (Larsch, et al, 2013). These tests can be used to refine the candidate

pool for successful drug therapies, which can then be scaled for mammalian studies, with the ultimate goal of reaching clinical trials in humans.

Currently, two methods exist for chemical screening applications using *C. elegans*. One of these methods is manual screening, which involves sequentially flowing different chemicals from a 96-well plate through a microfluidic arena containing *C. elegans*. The activity of these worms is either recorded on a behavioral level, using bright-field microscopy video recordings, or on a neurological level by imaging fluorescently labeled neurons. This is an effective method of microfluidic liquid delivery because it is relatively inexpensive (beyond the cost of the microscope, camera, and computer system), easy to conduct and troubleshoot, and adaptable (Giacomotto et al, 2012). However, because this method is conducted manually, it is susceptible to human error. This produces unrefined results, such as air bubbles and incorrect timing of chemical and liquid switching. By introducing air bubbles into the arena, the worms are not homogeneously exposed to the liquid, which can prevent them from coming in contact with the stimuli, ultimately altering the results. Similarly, because chemical screening is a systematic, time-dependent process, inserting the liquid into the arena too quickly or too slowly can affect the data collected and corrupt the results. Moreover, the experimenter has to be present for the entirety of the experiment, which poses problems with efficiency.

The other method of chemical screening, automation, can be accomplished through three combined major functions: pipetting, liquid delivery, and sorting. The Gilson PIPETMAX can transfer a tray of 96 pipet tips concurrently from one 96-well plate to another, thus only serving the purpose of mass-pipetting (Pipetmax). The BioTek MicroFlo is a fluid dispensing system that can be used to transport *C. elegans*, as the nematodes can be mixed into a liquid medium, but this only transfers *C. elegans* from the library to the microfluidic arena by means of liquid delivery

and does not address pipetting or sorting (Greene, 2007). The COPAS BIOSORT is a sorting machine that uses calcium imaging to read the degree of fluorescence emitted from test subjects. However, this imaging can only occur after the reagent has already been added and not during the uptake process, which limits its use in same-time automated monitoring (Copas). All of these devices are very expensive, on the order of at least tens of thousands of U.S. dollars, and each only executes one specific task. There is no standalone-automated system that carries out all three tasks of automation by itself, thus there is a need to create a system that can perform these functions, while dynamically monitoring neural activity in *C. elegans*.

We plan to create an automated system to improve the throughput of the chemical screening of *C. elegans* by alleviating the current drawbacks associated with these methods. Our system will use inexpensive, polydimethylsiloxane (PDMS) cast microfluidic arenas that are capable of holding many nematodes at once. We aim to combine the dynamic capabilities of manual screening with the precision and ease-of-use associated with more expensive, automated chemical screening devices. Our formal client statement is to design, develop, and assess an automated system to improve the throughput of neurological screening assays in *C. elegans* by sequentially delivering chemicals from a 96-well plate to a microfluidic arena. After developing the system, we will test it to ensure that all of the functional constraints are met. These include the prevention of air bubble entry, contamination, and incorrect timing of chemical switches. If the device falls short of meeting any of these requirements, we will revise the design accordingly. Once we have a working system, we will use it to conduct chemical screening experiments using the *C. elegans* nematodes.

Chapter 2: Literature Review

Here we present a thorough synthesis of relevant information collected in our research of neuroscience, *C. elegans*, and chemical screening. Specifically, we emphasize human neuropsychiatric disorders, their effects on the brain, and the implications of research in the field. We then discuss *C. elegans* and the nature of research conducted with these nematodes. We conclude by explaining a specific venue of neuropsychiatric disorder research, using chemical screening, and *C. elegans* as disease model experiments to facilitate drug discovery.

2.1 Neuroscience

In this section, we explain the general physiology of the brain, focusing on human neural anatomy and neurotransmitters. We then explain how irregularities in neurotransmitter systems can lead to neuropsychiatric disorders, chiefly schizophrenia and autism spectrum disorders. We subsequently transition from the effects these disorders have on sufferers to current treatment methods, as well as what current research is being done for the advancement of neuropsychiatric disease treatment.

2.1.1 Neurobiology

This section serves as a general introduction to the field of neurobiology. Emphasis is placed on human neural anatomy and processes.

The brain is the least understood organ of the human body, due to the complexity of both its anatomy and function. The brain is comprised of approximately 86 billion neurons, or nervous system cells, which communicate with one another through electrical and chemical signals (Azevedo et al., 2009). Neurons vary in function, chemical activity, and shape, but they generally contain the same fundamental cellular components. As shown in Figure 1 below, neurons

comprise a primary cell body (soma), axons, and dendritic projections. The cell body contains a nucleus and maintains the fundamental cellular functions required for the life of the cell (Squire, 2008).

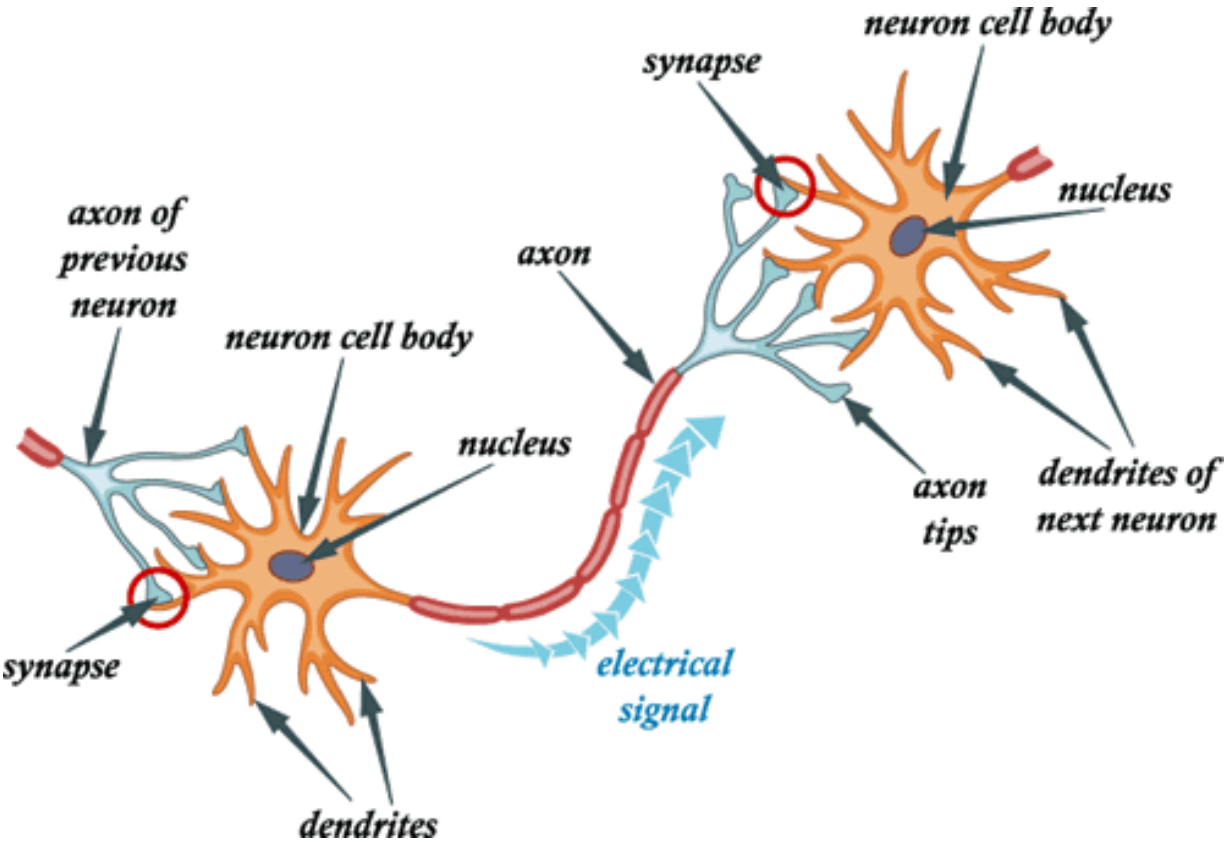

Figure 1: Neuron anatomy and physiology
(http://www.helcohi.com/sse/body/nervous.html)

There are three different classes of neurons in the body: sensory, motor, and interneurons (Bear et al., 2007). Sensory neurons are responsible for sensing things in the body's environment, and are also referred to as afferent neurons because they relay information inward, to the central nervous system (CNS). Motor neurons are required for the execution of actions, which can manifest as things like physical movement or secretion from glands (Bear et al., 2007). Motor neurons are also referred to as efferent, because they communicate information

away from the CNS. Interneurons bridge the gap between sensory and motor neurons, allowing them to interface with one another (Bear et al., 2007).

Neurons communicate with one another by sending electro-chemical signals via synapses and gap junctions (Bear et al., 2007). Chemical synapses are much more common in the CNS and have the ability to induce both excitatory and inhibitory responses. This form of neural communication is caused by the propagation of action potentials, which originate at the axon hillock (where the soma and axon meet) and travel through the axon to other neurons (Bear et al., 2007). This cascade of events results from the exchange of ions (sodium (Na^+), potassium (K^+), calcium (Ca^{2+}), and chlorine (Cl^-)) into and out of neurons through transmitter-gated (t-gated) and voltage-gated (v-gated) ion channels, which ultimately enables the release of neurotransmitters.

Neurotransmitters are signaling molecules that are synthesized in the cell body or axon terminal, packaged into synaptic vesicles, carried down the axon along microtubules (only the peptide molecules that are synthesized in the cell body), and released across the synapses present at the terminal end of each axon (the synaptic button, or axon tip as labeled in Figure 1) (Bear et al., 2007). Figure 2 below, illustrates the synaptic connection between two neurons, and the release of neurotransmitters across the synaptic cleft to interact with receptors on the postsynaptic neuron.

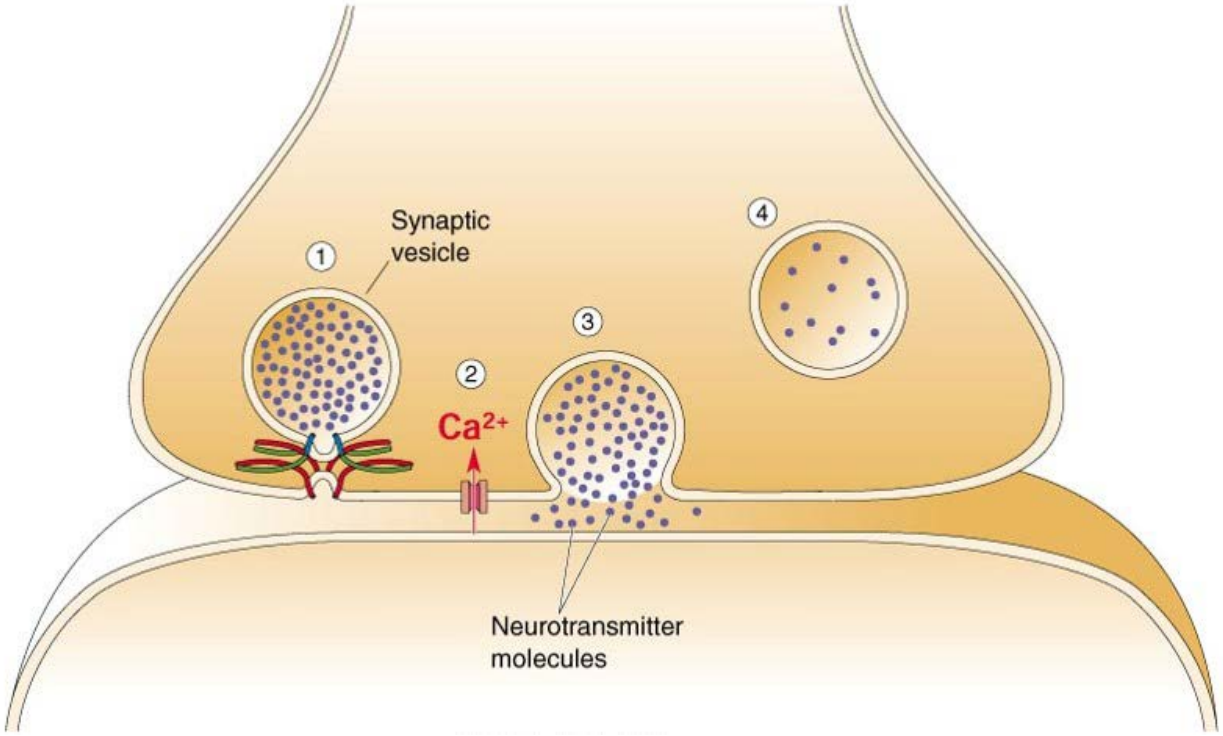

Figure 2: Release of neurotransmitter molecules across synapse (Bear et al., 2007)

There are two major classes of neurotransmitters: small molecule neurotransmitters and peptide neurotransmitters (Bear et al., 2007). The former class is divided into a number of different sub-categories that include: Acetylcholine, amino acids (e.g. glutamate, γ-aminobutyric acid (GABA), glycine), purines (e.g. ATP), and biogenic amines (e.g. dopamine, norepinephrine, and serotonin (5-HT). (Purves, Augustine, Fitzpatrick et al., 2001). These signaling molecules play important roles in a number of different neurological functions. The communication of neurons ultimately enables the body to sense internal and external environmental cues, and relays information to the brain and muscular system to allow for executed responses. Proper neurological activity is required for thinking, remembering, perceiving, controlling movements, and social interactions.

2.1.2 Neuropsychiatric Disorders

Abnormalities in the activation of voltage-gated ion channels in the central nervous system can directly cause abnormalities in "neurotransmitter release, neuron excitability, gene transcription, and plasticity." Specifically, "point mutations in calcium, sodium, and potassium channel genes" are highly associated with certain neuropsychiatric disorders, such as bipolar disorder, schizophrenia, and autism (Hyman, 2010).

Schizophrenia

Schizophrenia in particular is caused by definitive neurobiological abnormalities. More explicitly, the cerebral cortex deteriorates, "most severely in prefrontal and temporal regions." This thinning of the cerebral cortex is due to a decrease in dendritic branching in cortical neurons, and not because of cell death, as commonly believed. Additionally, cortical interneurons produce less GABA than necessary, thus establishing a major deficit of the brain's primary inhibitory neurotransmitter. Finally, hormonal and neurotransmitter imbalances in the midbrain neurons significantly contribute to schizophrenia, by means of "excessive dopamine release in ventral and perhaps dorsal striatal projections of midbrain dopamine neurons" (Hyman, 2010). This results in increased excitability of the midbrain neurons and thus alters motor control and hormone release as well.

To accurately gauge the importance of schizophrenia research, the worldwide lifetime prevalence, also known as the number of surviving individuals with the disease at any given point in time, must be clear. Although there is much variation between different geographic regions, social status, and sexes, McGrath et al. estimated the median lifetime prevalence of schizophrenia in all persons to be four per one thousand people, or about 0.4 percent of the population. Data from 46 countries were amassed, and an estimated 154,410 cases were

consolidated, ultimately yielding this comprehensive estimate of worldwide prevalence (McGrath et al., 2008).

Autism

As autism is a spectrum disorder, symptoms range from mild to severe, depending on which form of the disease the sufferer has. Kanner syndrome is a form of autism that manifests as mental retardation. This can cause frustration in sufferers, which can then become aggression. On the other side of the spectrum, Asperger syndrome is a form of autism in which sufferers generally have higher levels of intelligence than normal. Their motor skills tend to be uncoordinated, but most have exceptional musical ability and rote memory. Additionally, a defining factor in Asperger syndrome is an obsession with routine (Autism main symptoms, 2007). Comprehensively, autism causes behavioral and social hindrances, which manifest in difficulty communicating and uncomfortable social interactions (NINDS, 2009).

Autism, like schizophrenia, is primarily caused by abnormalities in neurotransmitter systems. Variations in ion channel genes cause abnormal levels of serotonin and similar neurotransmitters in the brain, which then alters the excitability of the neurons. This can be attributed to abnormal brain growth during fetal development of autistic persons (NINDS, 2009). Early brain overgrowth then would result in increased neuron numbers in the prefrontal cortexes of young children with autism. Additionally, the characteristic imbalances in neurotransmitters are coupled with irregularities in the immune system. This then leads to neuroinflammation, which is common in persons with autism (Lai, 2014).

Calahorro et al. estimate that roughly one percent of people have autism, but the rate of autism is rising, due to the fact that it is increasingly being recognized as a spectral disorder (Calahorro, 2011). Yeargin-Allsopp et al. reported the prevalence of autism spectrum disorders

in young children ages three to ten, in metropolitan Atlanta, which was 34 per 10,000 (Fombonne, 2003).

2.1.3 Drug Research

This section notes the current approaches being taken to treat these diseases in humans and the limitations that accompany them. This sets the stage for the clinical need for high-throughput drug discovery.

Schizophrenia and autism differ in that schizophrenia is a psychotic disorder, while autistic spectrum disorders are pervasive developmental disorders (PDD's) (Odle, et al., 2011). Psychotic disorders are widely treated with antipsychotic drugs, while PDD's can be treated with general psychotropics, e.g. "antidepressants, stimulants, antipsychotics, or anti-epileptics." Approximately half of patients suffering from PDD's are prescribed one or more of these medications (Santosh et al., 2001). Leucht et al. conducted a study testing the efficacy of antipsychotics against placebo, and the results distinctly indicated that treatments with antipsychotics have much lower relative risks than placebo, at 27 versus 64 percent (Leucht et al., 2012).

Although their efficacy has been widely tested and accepted as higher than that of placebo, antipsychotics have a number of side effects, namely weight gain and extrapyramidal side effects (Leucht et al., 2013). Extrapyramidal side effects are commonly involuntary muscle movement irregularities, such as dystonia, rigidity, hypokinesia/akinesia, dyskinesia, akathisia, and tremors/parasthesias. In layman's terms, these are the erratic increase in muscle movement and the dramatic decrease in muscle movement speed (Houltram, 2004).

These side effects, while coupled with efficacious treatments, are quite severe and barely manageable. If a treatment can be developed without causing such drastic side effects, the use of

such a drug would be relatively widespread. Thus, there is a need to research drug alternatives and test whether the efficacy can be improved and side effects can be minimized.

2.2 *C. elegans*

This section provides an introduction to *C. elegans* history, anatomy, genetics, and research applications. Additionally, their use as a model system for neurological studies is discussed.

2.2.1 History of *C. elegans* Research

This section serves as an introduction to C. elegans research, providing the reader with a fundamental understanding of how long this field has been in existence, and how it has evolved over the past 50 years.

Early research

C. elegans are roundworm nematodes that are naturally found in soil or decaying plant matter (Felix, 2010). Dr. Sydney Brenner began *C. elegans* laboratory research in 1963. He sought to use *C. elegans* as a model organism for biology and neurology research due to their rapid life cycle, simple reproductive cycle, compact genome, and microscopic size (Ankeny, 2001). Brenner used ethyl methanesulphonate (EMS) to mutate the *C. elegans* in order to test their behavioral response and survival rates. Experiments with EMS allowed Brenner to characterize 100 genes that were further mapped into six linkage groups (Ankeny, 2001). Brenner's preliminary research prompted further *C. elegans* experimentation, making it the first animal to have its entire neural network mapped, thus allowing them to be applicable in various types of genetic and neurological drug testing.

The earliest drugs testing techniques with *C. elegans* consumed large amounts of time and were labor and resource intensive. It was not until 2006 that *C. elegans* were used for a large scale high-throughput drug screen by Dr. Kwok and his colleagues to assess bio-activity of various compounds (Riley et al., 2014). As research progressed and methods for high-throughput experimentation were refined, scientists began utilizing *C. elegans* for drug discovery for neurological disorders due to their anatomy and simple genetic makeup (Ankeny, 2001).

2.2.2 *C. elegans* Anatomy

This section provides an anatomical overview of C. elegans, important for framing their usefulness in neurological research.

General anatomy

C. elegans nematodes are an ideal animal model for high-throughput biological research applications due to their size, life cycle, ease of reproduction, and anatomical and genetic simplicity. *C. elegans* are transparent, one-millimeter long worms that allow for easy laboratory maintenance. They can grow on agar plates or in liquid cultures with *E. coli* as a food source (Wood, 1987). Additionally, they mature to young adulthood in three days and live for approximately two to three weeks, given that they are under optimal temperature (20°C) and supplied with a sufficient amount of E. coli (Bono, 2005). Once they become young adults, *C. elegans* are able to reproduce, both sexually and asexually. Figure 3 below displays the *C. elegans* life cycle progressing from an egg to an adult. There is a point in the maturation cycle, after the middle of the first larval stage, where the *C. elegans* can enter an arrested development state called dauer, or the non-aging state. This is caused by two environmental factors – high temperature and lack of food (Riddle, 1988). *C. elegans* can survive up to four months during

this state of starvation and minimal mobility. The four-month dauer larva can be stored and utilized for future experimentation (Wormatlas, 2006).

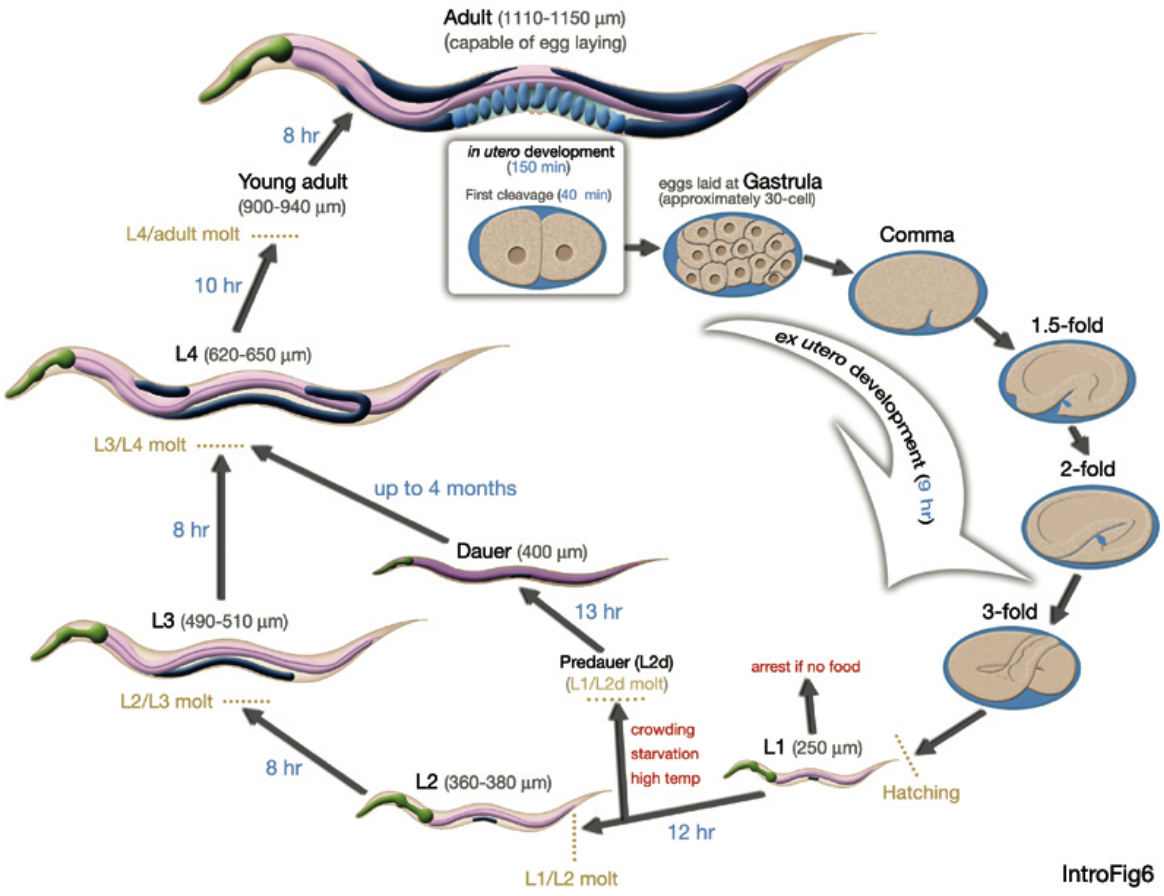

Figure 3: C. elegans life cycle with given durations during development

There are two *C. elegans* sexes, hermaphrodite (XX) and male (XO), as shown in Figure 4. Hermaphrodite *C. elegans* can self-fertilize, which allows them to produce genetically identical offspring as well as males. Hermaphrodite self-fertilization can produce 300-350 offspring, which is significantly greater during male fertilization (Wood, 1987). Furthermore, male mating simplifies the isolation and maintenance of mutated strains in the *C. elegans* (Anderson, 1995). The number of cells that make up *C. elegans* also depends on the gender; hermaphrodites contain 959 cells, while males contain 1031 (White, 1988). These cells comprise

the hypodermis, muscles, digestive tract, reproductive system and nervous system (Figure 4). The *C. elegans* transparent body also provides researchers with a visualization of the nematode's internal organs.

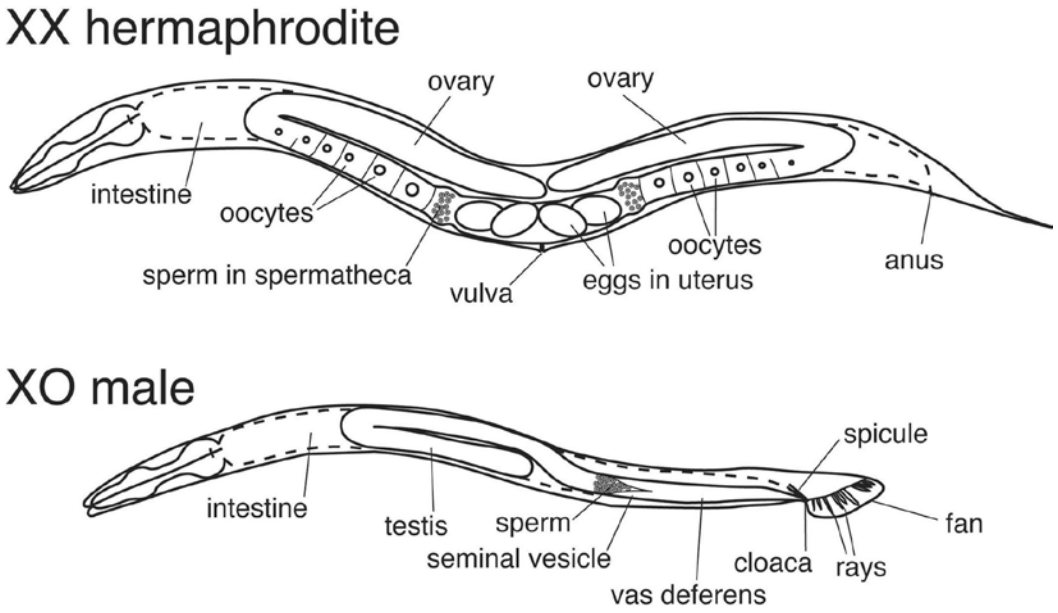

Figure 4: C. elegans genders, hermaphrodite and male, with respective anatomical structures (Wormbook.org)

Neural anatomy

In 1998, *C. elegans* became the first multicellular organism with a completely sequenced genome, comprised of 302 or 381 genomes, in hermaphrodites and males respectively. This breakthrough induced further research of *C. elegans* to enhance the biological understanding of all animals (Hope, 1999). The hermaphrodite's neurons can be grouped into 118 classes: 39 of which are sensory neurons, 27 motor neurons, and the remainder interneurons (Bono, 2005; White, 1988). The male *C. elegans* has 79 extra neurons (381 total), which are devoted to the male mating behavior (White, 1988). The neurons are predominantly located in the head around the pharynx of the *C. elegans*, as shown in Figure 5. In the body, there is also a continuous row of neurons at the midline and some scattered at the lateral parts of the body (Wormatlas, 2006).

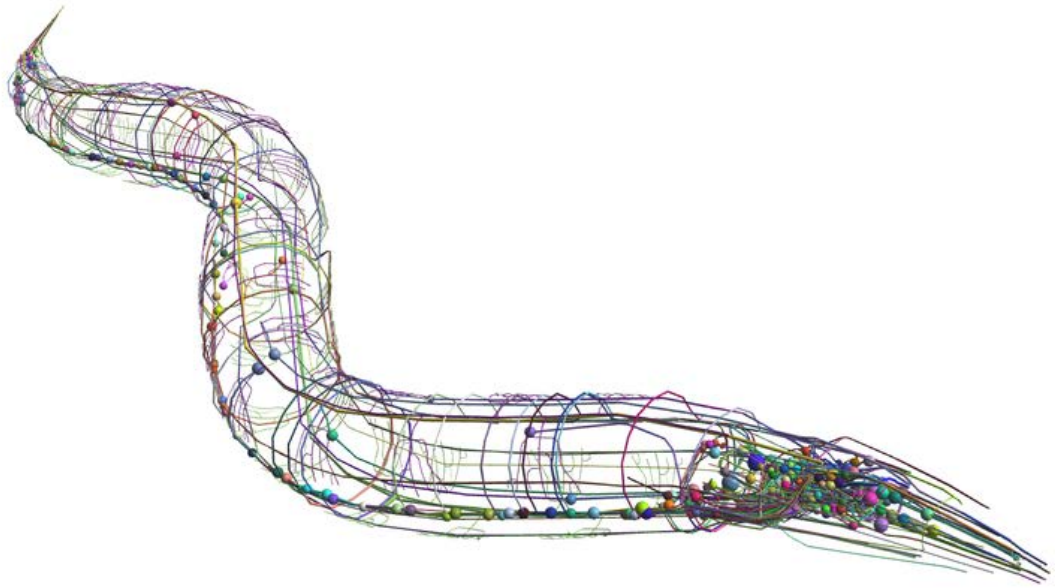

Figure 5: C. elegans neural network with each neuron location within the body.
(http://www.neuroinformatics2012.org/abstracts/the-neuroml-c.-elegans-connectome)

C. elegans with 302 neurons have approximately 5000 chemical synapses, 600 gap junctions, and 200 neuromuscular junctions (Bono, 2005; White, 1988). Additionally, common neurotransmitters have been assigned to *C. elegans* neurons. These neurotransmitters include acetylcholine, glutamate, γ -aminobutyric acid (GABA), serotonin, and dopamine (Bono, 2005). The synapse and neurotransmitter can determine the excitability and inhibitory response of *C. elegans.* The neural response can be studied when *C. elegans* undergo various stimuli (Riley et al., 2014).

2.2.3 Genetics

This section serves as an introduction to C. elegans genetics, illustrating how they can be used as models for human disease genes. This has significant research implications, in that C. elegans can open the door to rapid means of clinical research, and they provide a less complicated methodology than working with larger, more complex animals.

General Genetics

The genome of *C. elegans* is approximately 8 x 10^7 base pairs of DNA distributed across five autosomal chromosome pairs and either one or two sex chromosomes. This size is only about half that of *Drosophila* and is much smaller than the human genome, which is approximately 6 x 10^9. However, this is partially due to the number of repeated genes. In *C. elegans* the proportion of repeated genes is only 17 percent, while in humans the proportion of repeated genes is significantly higher at 50 percent (Wood, 1987). This results in about 50 percent *C. elegans* genes have a homolog found in the human genome. The proteome of *C. elegans* has a more significant homology with the human proteome at approximately 83 percent (Lai et al., 2000). This means that the proteins made by the genes in *C. elegans* are very similar to the proteins in humans, despite their drastically different levels of complexity and functionality.

The sex of a nematode is dependent upon the sex chromosome arrangement. If there is a pair of X chromosomes, the nematode is a hermaphrodite. Hermaphrodites are capable of self-fertilization by performing both spermatogenesis and oogenesis, the former of which occurs earlier in the life cycle. The other sex of *C. elegans* is a male with the ability to perform spermatogenesis. The sperm produced by males is able to inseminate the hermaphrodites. However, the population ratios do not favor the male sex, as fitness dictates that self-fertilization is more favorable. As such, less than one percent of hermaphrodite offspring is male. Additionally, when males inseminate a hermaphrodite the result is a 50 percent split between males and hermaphrodites (Gilbert, 2013). Therefore, it is easy to control the population to a desired sex.

Genetic Engineering Capabilities

The occurrence of recombination is found in oogenesis and spermatogenesis, in both males and hermaphrodites. However, due to the higher frequency of recombination in hermaphrodites, due to two sex chromosomes, the hermaphrodites have been studied more in depth. The rate of recombination increases with temperature and decreases with age of the nematodes (Wood, 1987). This means that spermatogenesis produces the most recombination early in the life cycle of a *C. elegans*. This takes place during the hermaphrodite's molting transitions to allow for oogenesis when it matures. Mutations usually occur on the autosomes and so those are targeted when genetically engineering nematodes.

One way to induce mutations is through the use of ethyl methanesulphonate (EMS). EMS is a monofunctional alkylating agent that has a rate of mutation of $5x10^{-4}$ per gene (Wood, 1987). There are a number of other mutagens for random mutation, but EMS was the most common due to it being a method from Brenner. Recent developments have been made in genetic engineering to insert genes into the *C. elegans* genome, which can be performed by utilizing the CRISPR associated protein 9 (Cas9) (Waaijers et al., 2013). Cas9 has the ability to target certain sequences in the genome and break the double strand of DNA to insert genetic information. While this method is a relatively new development, it holds promise for gene targeting success in the future.

2.2.4 Research Applications

This section provides an overview of different applications that C. elegans have been used for, demonstrating the tangible benefits as a model system.

C. elegans have proven to be an ideal animal model for high throughput screening in order to discover effective pharmaceutical therapies, chemicals, or even toxicology that have

neural or behavioral effects. *C. elegans* have been utilized for many high throughput drug discovery applications, thus replacing the labor and resource extensive cell based systems, due to their 60-80 percent homology to humans, genetic tractability, and versatility (Gosai et al., 2010; Riley et al., 2014). Various experiments have been conducted for drug discovery for neurodegenerative disorders such as Alzheimer's, Parkinson's disease, and Huntington's disease, amyotrophic lateral sclerosis, frontotemporal dementia, and spongiform encephalopathics (Gosai et al., 2010). Generally, these experiments are run with various strains of mutated *C. elegans* to mimic the symptoms of the specific disorder to accurately evaluate drug efficacy and absorption, distribution, metabolism, excretion, and toxicity (ADMET) (Riley et al., 2014).

C. elegans are also useful for various chemical genetics applications. Researchers are able to fast forward and reverse genetic tools to identify drug targets and understanding the mechanism of action of specific drugs using *C. elegans*. For example, feeding *C. elegans* with bacterial expressing dsRNA alter the *C. elegans* gene expression. This type of experimentation has induced genome-scale chemical genetics examination (Riley et al., 2014). Figure 6 below shows various types of *C. elegans* research methods including: morphology, locomotion, immobilized fluorescent imaging and live fluorescent imaging. Each of these methods would be applicable to different neurological and behavior studies. For example, the first instrumentation method listed would be for behavior *C. elegans* studies while, the second and third instrumentation methods would be for neurological *C. elegans* studies (Riley et al., 2014)

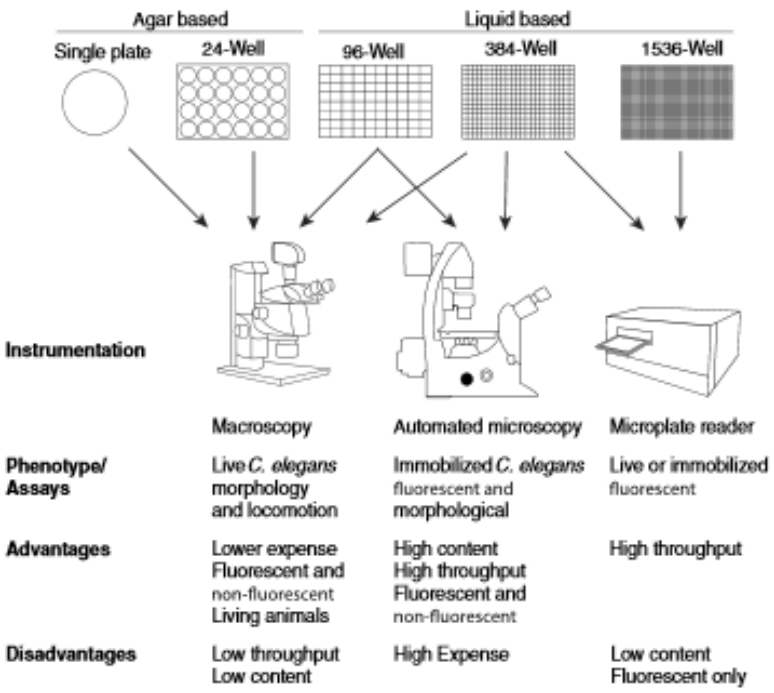

Figure 6: Various applications for C. elegans research including the instrumentation, phenotype/assays, advantages and disadvantages (Riley et al., 2014)

2.3 Chemical Screening

Chemical screening is a method for high-throughput experimentation, commonly used in drug discovery. Here we explain how chemical screening experiments are currently conducted, what methods are used, and what methods can be used in the future.

2.3.1 Manual Process of Chemical Screening for *C. elegans*

This section discusses the current system used for the chemical screening of C. elegans. Additionally, it includes an overview of the protocols used to create microfluidic arenas and conduct neural imaging (Ca^{2+}) experiments. Finally, a brief review of the mathematical models used to quantify neural responses is provided.

For current chemical screening applications using *C. elegans*, the gold standard for high-throughput behavioral and neurological studies is the manual screening approach. Described by

Larsch et al. and Lagoy & Albrecht, microfluidics are a useful way to record and analyze *C. elegans*. This method involves the use of transparent, polydimethysiloxane (PDMS) microfluidic devices to house *C. elegans*, which provide complete visualization of the worms. These devices allow for the collection of data from a large number of animals, as some devices are capable of housing up to 100 nematodes. Additionally, they can be used with both bright-field and fluorescent microscopy, enabling the study of behavioral and neurological responses, respectively. Pure laminar flow and the minimal amount of liquid contained in these devices allows for rapid and reliable switching of liquid stimuli.

The process of fabricating PDMS devices is relatively inexpensive and can be used to produce arenas with varying features. The process begins with soft photolithography microfabrication to create a silicon wafer master mold, which is described by previous methods (Larsch et al., 2013). The physical process of producing a silicon master is minimally time consuming (2-3 hours), however the creation of photomasks with the correct dimensions can take many iterations. Fortunately for our applications, optimal photomasks for the production of devices to study young adult *C. elegans* have been developed. Upon completion of the microfabrication protocol, PDMS mixture (10:1 ratio of polymer-to-crosslinking agent) poured over silicon wafer in a large diameter petri dish, degassed, and baked to elicit crosslinking (Lagoy & Albrecht, 2014). Devices are then cut out of the dish using a scalpel and carefully separated from one another along borders using a razor blade. Inlet, outlet, and worm loading ports are created using a 1mm dermal punch. These methods have been previously described by Lagoy & Albrecht, and a schematic of the PDMS device fabrication is shown below in Figure 7.

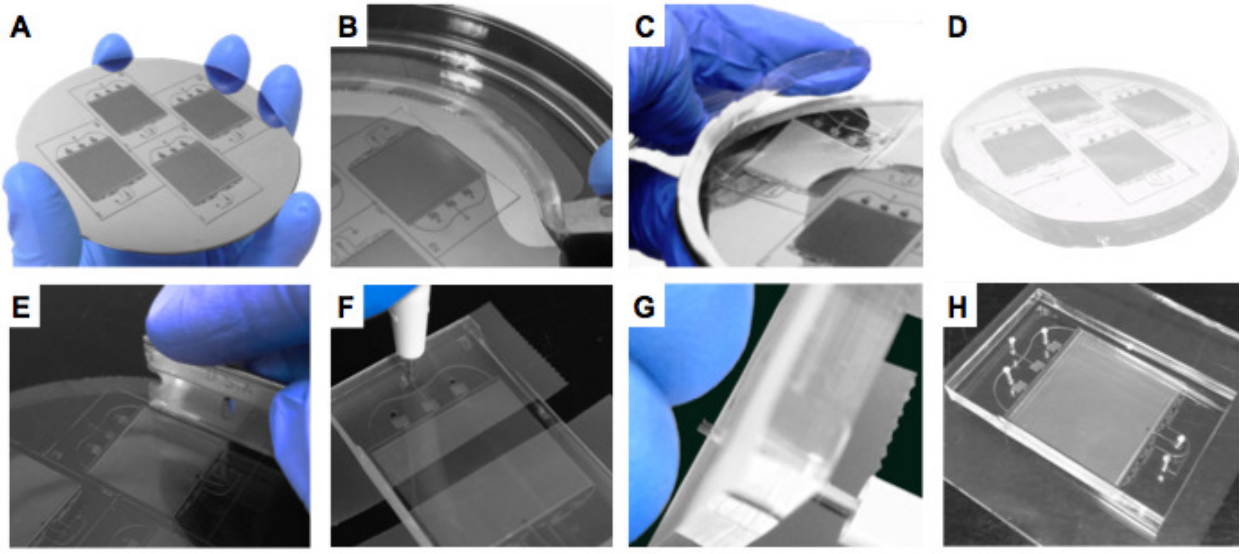

Figure 7: Polydimethylsiloxane (PDMS) device fabrication (Lagoy & Albrecht, 2014)

Once the devices are cut out from the complete PDMS mold and punched, they are washed using ethanol and water, and dried with compressed air. They are then placed between a fluorinated piece of glass (arena side of PDMS) and an untreated piece of glass (top side of PDMS device), sealed using a clamp system, and degassed prior to conducting experiment (Figure 8).

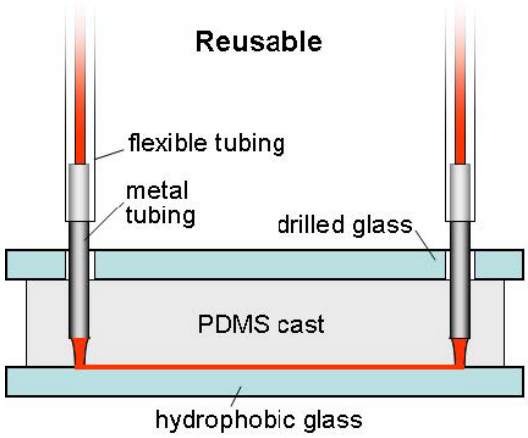

Figure 8: PDMS device for experimental use (Lagoy & Albrecht, 2014)

For screening applications, chemical stimuli are drawn by gravity through the microfluidic arena containing *C. elegans*. This setup involves pipetting liquid chemicals into the wells of a 96-well plate, loading the worms into the arena, establishing flow of the chemicals through the device, and recording the behavior or neurological responses using a microscopic camera (Larsch et al., 2013). A schematic overview of this system is displayed in Figure 9 below.

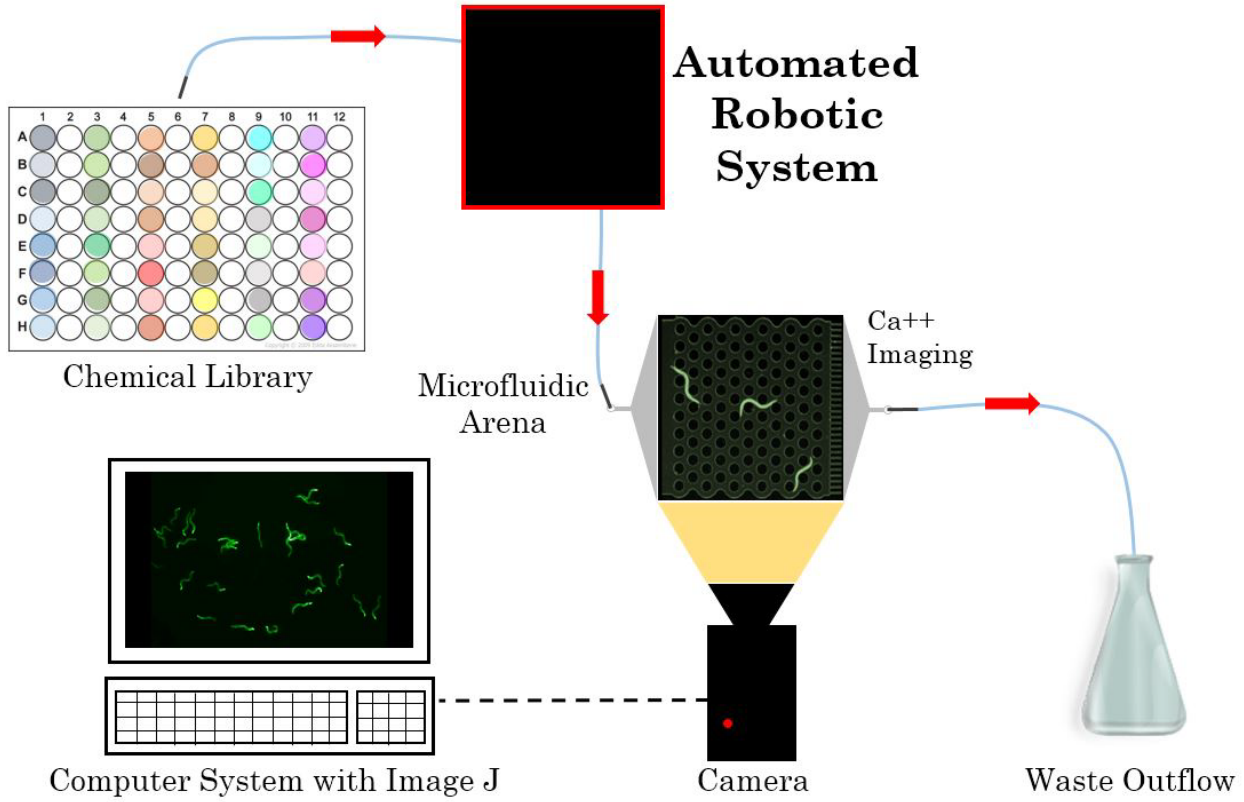

Figure 9: Schematic of manual chemical screening assay

Depending on the use of bright-field or fluorescent microscopy, the behavior or neurological responses of *C. elegans* can be recorded for computational analysis. For behavioral studies, the movement of worms can be analyzed using MATLAB, and the average behavioral responses to chemical pulses, stripes, and gradients can be quantified (Larsch et al., 2013). The chemical screening method that our project aims to augment with an automated robotic system,

involves the quantification of neural responses to a library of chemical stimuli. As previously reported, ImageJ, which is a scientific image analysis software developed by the National Institutes of Health (NIH), can be used to assess the intensity of fluorescently labeled neurons in *C. elegans* (Schneider, 2012). This is used to study dynamic calcium activity in the neuron of interest, which indicates the signaling activity of the cell/neural pathway. As shown in Figure 10 below, the neural activity of each particular animal can be distinguished, which allows for the establishment of a baseline of fluorescent intensity for each worm (Larsch et al., 2013). This baseline is important for determining the overall change of intensity, thus the varying degrees of response between different worms.

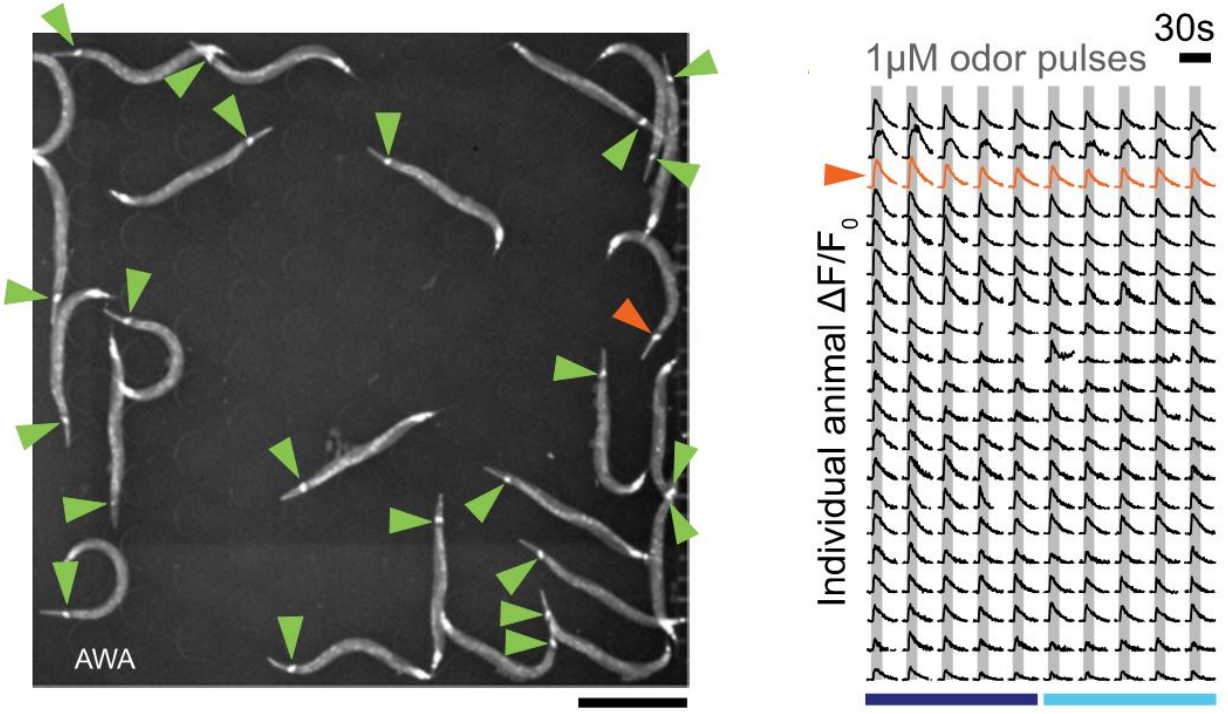

Figure 10: ImageJ analysis of calcium activity of C. elegans AWA neuron in response to 1μM diacetyl (Larsch et al., 2013)

For the images analyzed in Figure 10 above, the worms were paralyzed using a drug called tetramisole (Larsch et al., 2013). The inclusion of this paralyzing agent allows for better neural analysis using ImageJ, because the worms move very little, making it easier to

consistently distinguish them from one another. While this method provides more stable data collection, it is not ideal due to the somewhat unknown additional effects of tetramisole, as well as the prevention of free movement. One of the greatest advantages of utilizing microfluidics for *C. elegans* research, is that their behavior can be assessed in a systematic manner; paralyzing the worms is somewhat contradictory to the overall goal of being able to study worms in as close to a native environment as possible. Calcium imaging tracking software, NeuroTracker 1.0, was developed in an attempt to overcome the problems associated with tracking the neural activity of freely moving *C. elegans*. This system was accompanied by a number of limitations, including large generation of data and the inability to distinguish worms from one another, both of which pose problems for high-throughput applications (Cupido, Feng, & Hess, 2014). To address these issues, the previous MQP developed a revised code called NeuroTracker 2.0, which allows for improved automation and enables the collection of neural data from up to 20 freely moving *C. elegans*.

Together the manual system for chemical screening and NeuroTracker 2.0 provide a good setup for high-throughput drug discovery research using *C. elegans*. The major limitation with this system is the reliance on manual operation of the chemical switching, which our design aims to augment.

2.3.2 Automated Systems

This section reviews the automated systems, both for liquid handling and C. elegans research, which have been explored.

Existing systems for automated fluid delivery

The existing systems for automated fluid delivery are expensive, designed to only transfer liquid, and are not easily modified. For example, the Precision Microplate Pipetting

System from Biotek, which uses eight pipetting tips that are able to fill a 96-well plate from a single reservoir (Larson, 2012). After the system is programed, it can be unattended for the duration of the liquid delivery to the desired plate. The system is able to dispense liquid, mix within the well (similar to a micropipettor), conduct serial dilutions, and transfer samples from one plate to another. The system is not able to transfer liquid to non-96 well plate containers, which means it is not capable of transferring to a microfluidic arena. The main drawback of the current systems on the market is that they focus only on transfer to a plate of wells and not to various containers. Additionally, the Precision Microplate Pipetting System is very expensive at $20,000.

Existing systems for automated *C. elegans* research

C. elegans are commonly studied due to their desirable characteristics (mentioned above), and there are a number of automated devices that have been designed to automate *C. elegans* analysis. One such apparatus is the BioTek MicroFlo, which is traditionally used to dispense specific volumes of liquid into a well plate. Although, it has also been used to dispense nematodes into a 96-well plate from a reservoir (O'Reilly, 2014). This system is beneficial because it is able to sort *C. elegans* in an automated fashion. However, it is not able to analyze them by any means. Additionally, the MicroFlo is also expensive, costing $13,000 on the secondary market.

One of the best devices on the market for analysis of *C. elegans* is the COPAS BIOSORT (O'Reilly, 2014). The BIOSORT is able to sort nematodes based on a number of parameters. By drawing from an entire population, the system is able to sort *C. elegans* based on size, number, and the fluorescence intensity. This system is ideal for monitoring the fluorescence of treated neurons in *C. elegans*, but the results are passive, only measuring how a reagent affected the

nematode at the peak of response. Essentially, the active uptake of a reagent cannot be seen, limiting the experimental results. Another drawback is the price for sale for $300,000.

One last method used to sort *C. elegans* is a modified use of fluorescence-activated cell sorting (FACS) (O'Reilly, 2014). As the name implies, this method is typically used for sorting fluorescent cells. A novel method has been developed to modify existing systems to sort *C. elegans* larvae based on fluorescence, which is called live animal fluorescence-activated cell sorting (laFACS). FACS is able to sort up to 100,000 larvae in one hour. This is beneficial because one can use the same system to sort cells and *C. elegans* larvae instead of having different systems dedicated to each. However, a drawback is the size limitation, which only allows young larvae to be sorted, as the system is traditionally just used for cells.

2.3.3 Arduino System

This section introduces the Arduino microcontroller and software environment. It serves to relate our literature review to our project strategy, indicating the methodological route we will take.

The Arduino prototyping device "is a microcontroller development platform paired with an intuitive programming language that you develop using the Arduino integrated development environment (IDE)" (Blum, 2013). The software is based off of C/C++, and it sets the stage for writing a computer program, which can then be uploaded to the Arduino board.

The hardware board is based off of an 8-bit Atmel AVR microprocessor, an oscillator, and a voltage regulator; it "processes inputs and outputs between the device and external components" that can be attached to the device (McRoberts, 2013). Adding separate components to the system can transform this device into a dynamic, programmable control unit for almost any application. Some external companies, including Adafruit, TinkerKit, Annikken Andee, and

Xbee, are approved by Arduino as viable producers of Arduino-compatible technology, and they even have products for sale through Arduino's site (Shields/3rd Party). These extra components, called "shields," are attachable circuit boards that add robust functionality to the Arduino project (McRoberts, 2013).

In addition, the Arduino is fundamentally open source, meaning "all the design files, schematics, and source code are freely available to everybody." Furthermore, it means that the Arduino software and hardware can be readily integrated into independent projects that steer away from the standard design protocol, and commercial distribution of these projects using Arduino's designs is permitted (Blum, 2013).

Since Arduino is a comprehensive and open-source product, its applications can vary greatly. Automation is well within Arduino's capabilities in terms of mechanical and electrical functionality. Arduino's online community, with its wide-reaching audience, will have the proper resources for our team to be able to find a suitable route for creating an automated chemical screening system.

Chapter 3: Project Strategy

The overall goal of this project is to create a device that enables the automated delivery of a chemical library to a microfluidic arena containing *C. elegans* nematodes. The purpose of this system is to facilitate high-throughput drug discovery for the treatment of neuropsychiatric disorders, which can be modeled using this organism. Moreover, we hope that this platform technology can be applied to other biological research, providing an automated alternative to applications such as cell culture studies, and staining. Using our background research and input from our project advisor, Dirk Albrecht, we have identified the following objectives and constraints to develop an approach to the task at hand.

3.1 Client Statement

At the onset of this project, our initial client statement was to: *Create an automated system to improve the throughput of microfluidic experiments using C. elegans.* After discussing the scope of the project with our advisor, and determining the current state of chemical screening in *C. elegans*, we revised our client statement to be to:

Design, develop, and assess an automated system to improve the throughput of neurological screening assays in C. elegans by sequentially delivering chemicals from a 96-well plate to a microfluidic arena. The system must deliver chemicals with a minimum flow rate of 0.1mL/minute and switch chemicals within one minute or less, while preventing the introduction of air bubbles. Additionally, the system must fit within the geometric confines of the current imaging apparatus.

This revision more clearly states the scope of our project, specifically with the addition of "assess," "neurological screening assays," "sequentially delivering chemicals from a 96-well

plate to a microfluidic arena", and the specific constraints associated with sequential delivery. The constraints given to us by our advisor provide minimum specifications that our system needs to achieve. Assessment of our system will increase the credibility of our project, since ensuring that the design actually works is essential to its scientific and commercial validity. Distinguishing the microfluidic experiments as "neurological screening assays" defines the experiments for which the system is intended, thus helping us tailor our system specifically to these experiments. The inclusion of "sequentially delivering chemicals from a 96-well plate to a microfluidic arena" clarifies the particular process our system aims to augment. With this goal in mind, we identified the following objectives and constraints, which provide a framework for the creation of an optimal design.

3.2 Objectives

Creating central objectives helped guide us in the design process. The objectives are outlined and categorized as follows: accurate, efficient, precise, safe, and user friendly. An objectives tree is shown below in Figure 11, which summarizes what we hope to accomplish by keeping each objective in mind throughout the design process.

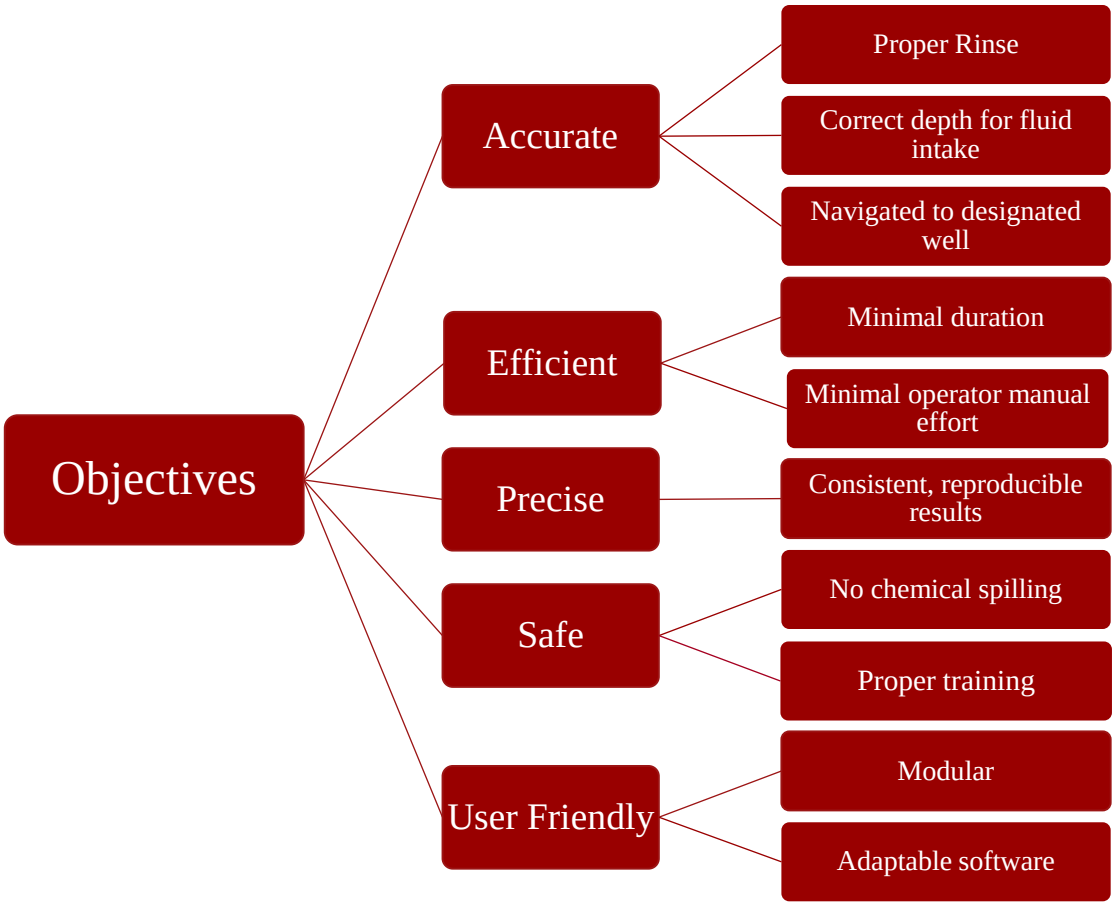

Figure 11: Objectives tree containing the primary and sub-objectives

To determine the importance of each objective in our design process, the objectives were ranked in a Pairwise Comparison Chart (PCC) (Table 1 below). After establishing a thorough description of each objective, the team began comparing them. Accurate received the highest ranking in the PCC, emphasizing the significance it has in our project. Our system has many accuracy specifications that will determine the quality of its performance while running experiments. The second highest ranking objective is precise. It is important for our system to be precise so that experiments can produce consistent and reproducible results. The third ranking objective is efficient. The efficiency of the system is less important than accuracy and precision because this objective caters to the convenience of the operator rather than to the functionality of the system. However, ideally the system will be hands-off with minimal effort for the operator.

The lowest ranking objectives are safe and user friendly. Safety is always a concern when working in a laboratory, but we predict our system will not pose any danger to the operator. Finally, the user friendliness of the system is not as important as its overall efficacy. Our advisor, Professor Albrecht, discussed the importance of our objectives and helped us refine our rankings. The PCC analysis of our objectives establishes a foundation for further development of our design process.

Table 1: Pairwise Comparison Chart (PCC) for ranking the five primary objectives

Objectives	Accurate	Efficient	Precise	Safe	User Friendly	Total
Accurate	X	1	1	1	1	**4**
Efficient	0	X	0	1	1	**2**
Precise	0	1	X	1	1	**3**
Safe	0	0	0	X	0.5	**0.5**
User Friendly	0	0	0	0.5	X	**0.5**

3.2.1. Accurate

In order for this system to be used for the collection of high-throughput neural imaging data, accuracy is imperative. For this project, accuracy means that the system remains error-free in its delivery of chemicals from the 96-well plate to the microfluidic arena. Thus, the automated chemical switches must be executed in a systematically reproducible manner. To generate viable results, the switches from one well to the next need to be controlled in an accurate spatial pattern to ensure that the chemicals are delivered in the intended order, with proper rinsing between different chemicals to prevent cross-contamination and a complete flush before the collection of data for each new chemical. Furthermore, the system needs to achieve the correct depth in the

2mL well to allow for 20 minutes of fluid delivery, without the introduction of air bubbles into the arena.

In summary, the sub-objectives that are encompassed by accuracy are listed below, ranked in order of importance (most important → least important). The sub-objectives were ranked based on our advisor/client's directives.

a. Navigates to a designated well under given commands
b. Properly rinses between chemical switches
c. Reaches correct depth for fluid intake

3.2.2. Precise

In order for our system to be used for viable data collection, it needs to be precise. For this project, precise means that the system must generate consistent, reproducible results. The experiments we conduct using the system must yield results that all fall within a reasonably narrow quantitative range, thus exhibiting statistical precision.

In summary, there is only one sub-objective that is encompassed by precision, which is shown below.

a. Consistent, reproducible experimental results

3.2.3. Efficient

To optimize the automated throughput of the system, it needs to run experiments in an efficient manner. Due to the time-consuming nature of manual chemical screening experiments, a key objective is that this system requires minimal user intervention after setup. As opposed to the current method, which requires the operator be present to execute the chemical switches by hand, an automated system would allow the operator to focus on other tasks during the

experiment. Additionally, it is also important to minimize the time required for each chemical switch, as this prevents wasting time that could otherwise be used to collect neurological data from the worms. Prolonged chemical switches do not have a negative effect on the validity of the data, but it decreases the throughput of the system.

In summary, the sub-objectives that are encompassed by efficiency are listed below, ranked in order of importance (most important → least important).

a. Minimize time the operator spends on the experiment
b. Minimize duration of chemical switching

3.2.4. Safe

In our system, safety is an important aspect. If the system poses a direct threat to the wellbeing of the operator, its practicality becomes questionable. Because of this, we plan for our system to be safely operable for any user, whether they are learning how to use it for the first time or have already mastered using it. This will be accomplished by ensuring that the system will not cause chemical spills through normal use, which could pose harm to the operator. Additionally, with moving parts there is always a heightened risk of mechanical failure, but for our design we plan to minimize the chance that such a malfunction could cause a chemical spillage. Furthermore, we will require that all users go through safety training before using the system, thus reducing the likelihood of improper use. By minimizing the risk of chemical spillage, mechanical failure, and improper use, we hope to prevent harmful outcomes due to operating this system.

In summary, the sub-objectives that are encompassed by safety are listed below, ranked in order of importance (most important → least important).

a. No chemical spilling

b. Proper user training

3.2.5. User Friendly

Ease of use will ensure that our system is competitive with similar products that are commercially available. The only parts of this setup that need to be changed from one experiment to the next are the 96-well plate, the PDMS arena with *C. elegans*, and the waste container. Changing these parts will be very intuitive so that proper setup is logical. Additionally, the software that will control the apparatus will also be easy to use and customizable so that the running of experiments will not be cumbersome.

In summary, the sub-objectives that are encompassed by user friendly are listed below, ranked in order of importance (most important → least important).

a. Ease of setup

b. Adaptable software

3.3 Constraints

As outlined by our advisor, the four categories of design constraints are physical, financial, efficacious (or experimental), and temporal. The only physical constraint is that the design must fit within the geometric confines of the existing imaging apparatus in Professor Albrecht's lab. Since we will be designing moving components that will attach to an existing apparatus, we must take precautions so as to avoid collisions of any components of the system with the existing apparatus.

The only financial constraint is our budget of roughly $500.

For efficacy, there are four distinct constraints. Switching between each individual chemical well must occur within one minute; furthermore, when switching between each chemical, a 0.01% carryover rate is the highest value that is acceptable for our purpose, since mixing multiple chemicals together can corrupt the collected data. Air bubbles must be prevented from entering the microfluidic arena during each chemical switch, so that there are no random gaps in the stimuli. Additionally, each individual 2 mL chemical well must last for 20 minutes, so the system must allow for a minimum flow rate of 0.1 mL/minute.

Lastly, the temporal constraint is that we finish the entire project within the allotted MQP timeframe. Table 2 below shows a visualization of the categorization of these constraints.

Table 2: Constraints organized into categories

Financial	• Budget must not exceed $500
Physical	• Must fit within the geometric confines of the imaging apparatus
Efficacy	• Chemical switching must occur in less than 1 minute • Allow for a minimum flow rate of 0.1 mL/minute • Air bubbles must be prevented during chemical switch • 0.01% chemical carryover across wells
Time	• Finish within MQP timeframe

3.4 Project Approach

In order to accomplish the goals set out for this project, we devised a project approach to which we plan to adhere. We have separated our project goals into two categories: design and validation. The design component of our project includes completing the existing microscope apparatus in Dr. Albrecht's lab. This involves constructing a method of chemical extraction from the 96-well plate by means of z-axis motion; the x- and y-axis components to the motion

involved in chemical extraction from the 96-well plate have already been designed and created by Dr. Albrecht.

The 96-well plate is attached to the apparatus using an aluminum holder that we developed, and is moved in a Cartesian-coordinate system, in the plane parallel to the lab floor, using Arduino software and a DC stepper motor. The chemicals should then be extracted from the plate using rigid tubing and height difference, to manipulate the liquid to move downwards into the arena. We use Arduino-controlled components to carry out this z-axis motion, since the x- and y-axis components were both already operating through the same technology. We believe using Arduino technology for all movement involved with chemical extraction streamlines the design and use of the apparatus as a whole.

The validation portion of our project involves conducting initial experiments to ensure that the apparatus meets all of the fundamental design objectives and constraints. Following this preliminary assessment, we will conduct previously studied neural screening experiments, to ensure that this apparatus is able to reproduce the results obtained using the existing methods. We hope that after the completion of our project, the overall experience and results of conducting high-throughput chemical screening experiments using Dr. Albrecht's apparatus will be more robust, hands-off, and reliable than through the current manual method.

Chapter 4: Alternative Designs

Using our objectives, constraints, and project approach that we previously outlined, we began the process of bringing our device to fruition. We researched potential pieces and methods that can be used to complete the apparatus, in accordance with the previously established functions, needs, and specifications. We brainstormed alternative designs and compared them to each other, weighing out the advantages and disadvantages of each, in order to decide upon a final design concept. We then modeled the physical setup of the apparatus as a whole in SolidWorks to ensure that everything would fit together and move properly. Finally, we discuss the experiments we will conduct to ensure that the apparatus closely follows the guidelines previously set for our design, while still maintaining functionality.

4.1 Needs Analysis

In terms of the results of our design and the preferences associated with them, set by our advisor, the experimental constraints are the "needs" of our design. To reiterate, switching between each chemical must occur in less than one minute, the setup should allow for a minimum flow rate of 0.1 mL/minute, air bubbles must be prevented during chemical switches, and there must be no greater than 0.01% chemical carryover across the wells. After meeting with our advisor, it was clarified that chemical switches must actually occur within a matter of seconds, and not just within one minute. Therefore, we sought to find a robotic component that prioritizes speed and accuracy of movement, in order to accommodate for this slight change in constraints.

As for the "wants" of our design, these are the experimental objectives we previously outlined. These entailed that the apparatus and the experiments carried out are accurate, efficient,

precise, safe, and user-friendly. Table 1 and Table 2 display visual representations of the relative importance of these characteristics.

Additionally, in order to complete the apparatus, our team has to design a platform that will hold the 96-well plate when it is going through chemical switching. To do this, we need to think about how this piece will fit into the overall apparatus spatially and then we will create a model using SolidWorks computer-aided design software, so that we can analyze how the different parts will fit and move together. As delineated by our advisor, this holding platform cannot be heavy, should not deform easily, and must have as little ground clearance as possible between the microscope platform, to minimize the tube length at the 96-well plate/microfluidic arena interface. Therefore, we will need to find materials and a design that fit these criteria.

4.2 Conceptual Designs

The final design was heavily dictated by the experimental constraints and suggestions from our advisor. At first there were a number of ideas that made use of different methods and were analyzed, but as the constraints became more defined the design took a more definitive shape. At the outset, since the x- and y-axis components were already constructed using Arduino hardware and software, we considered using the same technology for the z-axis motion ideal. However, since these components were already constructed, it left us with a limited space to work within.

The 96-well plate holder could not be higher than the moving platform, so we decided that a two-piece holder secured together by screws was the best design. This was intended to limit the amount of material needed, and allowed for more structural integrity, compared to soldering two pieces together.

Next, we analyzed the method by which to obtain the liquid from the 96-well plate through the z-axis. This component must accommodate rigid tubing, for fluid delivery from the 96-well plate to the microfluidic arena, and perform fast chemical switches, as stated in the constraints. Our design options for the z-axis motion, along with explanations of our decision processes for each, are detailed below. For each option, we wanted to capitalize on the design objectives we described previously, while keeping our constraints in mind.

Linear Actuator

With rigid tubing and the need for quick switching, we posited that a miniature linear actuator would be ideal to move the tubing. However, the commercial options available for this device were limited in options for length and speed. Moreover, it is expensive and very heavy, so we opted to find different design ideas. A visual representation of this design is shown below in Figure 12.

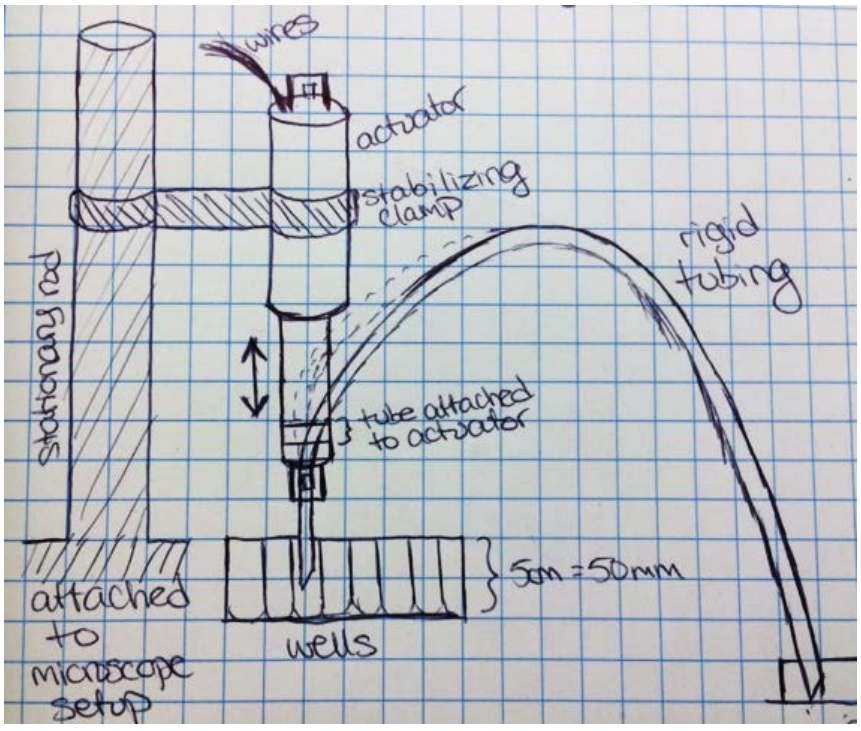

Figure 12: Conceptual drawing of the linear actuator

Elevating Platform

We considered an elevating platform, which essentially was a lab jack placed on top of the 96-well plate holder, and underneath the plate itself. This eliminated any need for attaching the tubing to any moving part, since the x-, y-, and z-axis movements would all be controlled by the motion of the plate. However, this was also a very bulky design and we feared it would increase the risk of chemical spills onto the apparatus, since the entire plate would be constantly moving. Additionally, this component is a rather costly one, so if we chose to pursue the idea, we would design our own 3D-printed version in Solidworks and have it machined in steel or aluminum. Still, this would be heavy and thus susceptible to excessive spillage since such large parts would be moving rapidly in each axis, seen below in Figure 13.

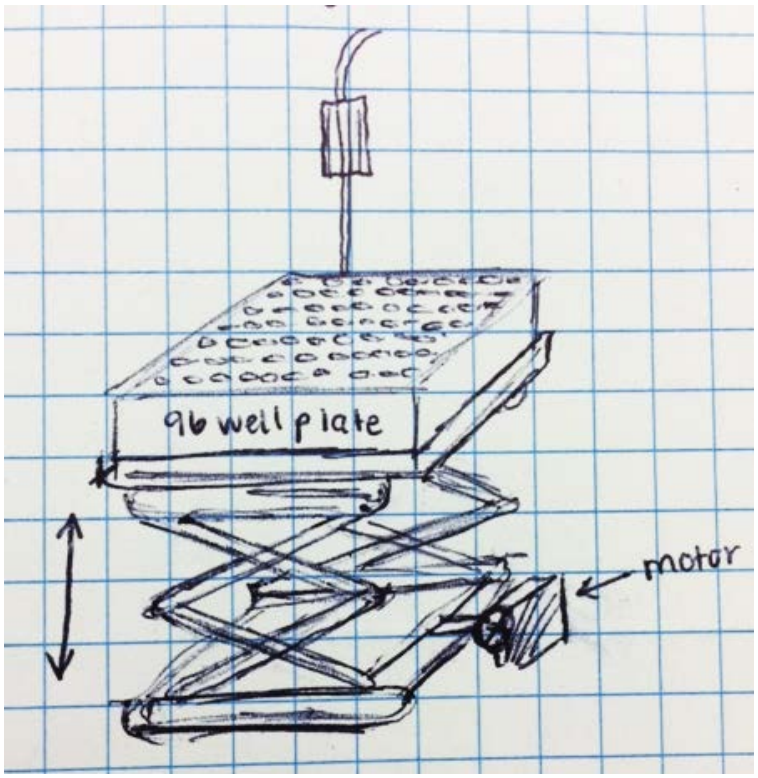

Figure 13: Conceptual drawing of the elevating platform design

Rotating tire

The rotating tire design includes the use of one servo motor and two tires. This design will be oriented horizontally and feed the tubing in-between the two rotating tires. The servo will control the movement of the tubing. The tubing will also be held in place on the base of the design to prevent it from moving out of place on either side. The conceptual drawing of this design can be seen below in Figure 14. This design will be inexpensive, however it is likely to be inaccurate.

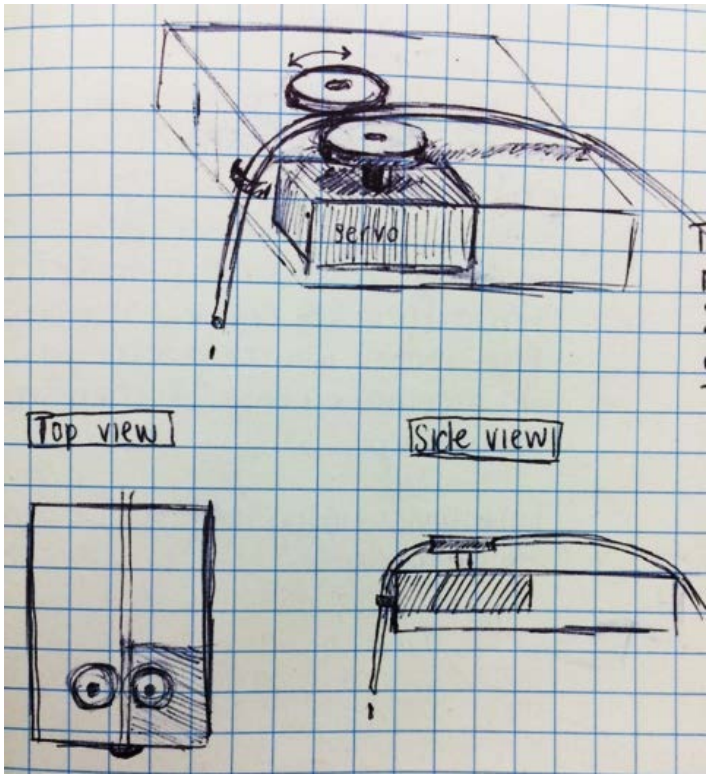

Figure 14: Conceptual drawing the rotating tire design

4-Link Hinge

The 4-link hinge design will include four joints and a servo motor. As the servo motor rotates 180 degrees at a fixed link it, will force the other links to move accordingly (up or down at the same degree), seen in Figure 15. The tubing will be attached to the moving links and sway under the given servo commands. This design will be inexpensive, but the swaying of the tubing will cause inaccurate movements.

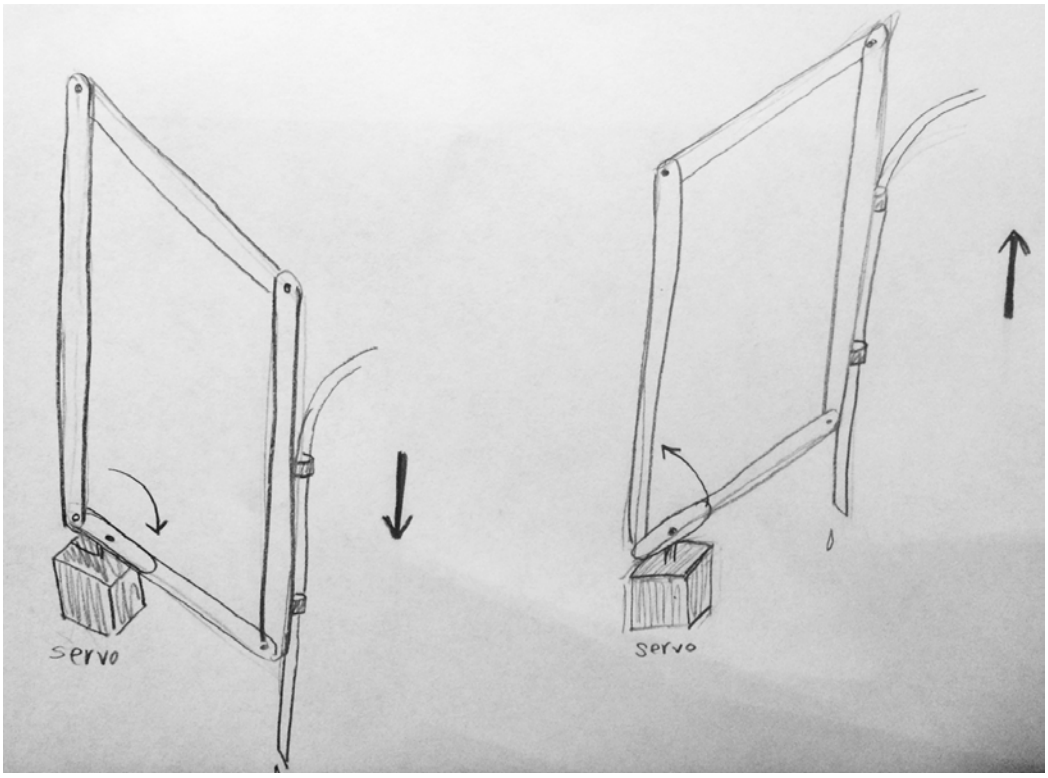

Figure 15: Conceptual drawing of the 4-link hinge design

Screw

We also considered the screw design, which includes the use of a stepper motor and various machined parts. The stepper motor would spin the threaded “screw” machined component in order to move the attached “nut” component up and down. The tubing will be attached to the “nut” part of the design and held vertically in a casing, Figure 16. We analyzed this design and it will be expensive with all of the custom parts and will need a lot of testing prior to its use.

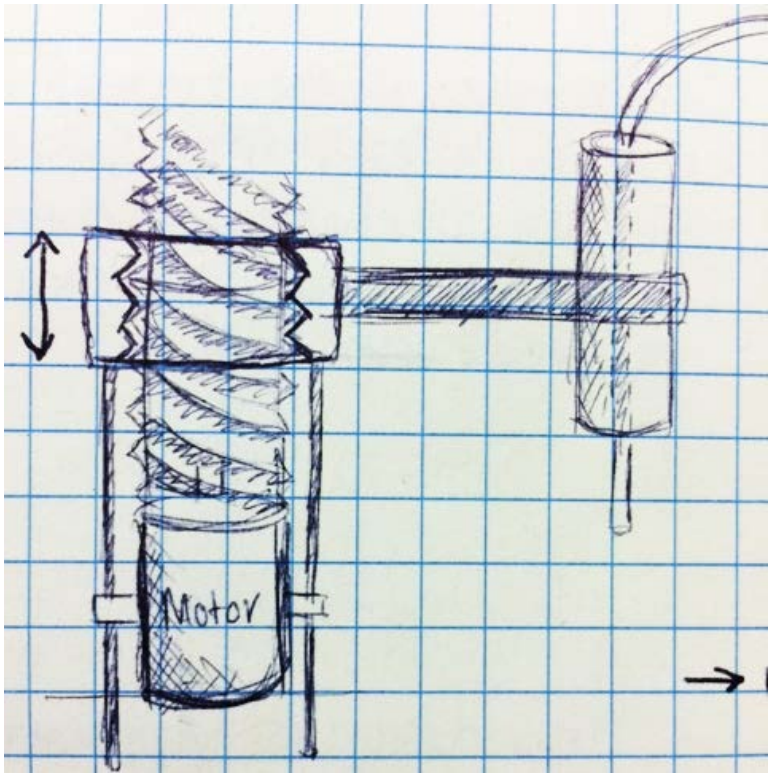

Figure 16: Conceptual drawing of the screw design

Pulley

We also analyzed the design concept of a pulley, with a belt running around two separate wheels arranged along the z-axis, and the tubing attached at two points along the belt in order to secure it, but not force it to snap, seen in Figure 17. The movement of the wheels would be controlled by a micro servo motor, which is very fast and inexpensive. Overall, this design would be very tall, consuming a considerable amount of space along the z-axis, but not as bulky in terms of surface area in the x- and y-axes. Moreover, the micro servo motor itself is very light, and the accuracy of its movement is high.

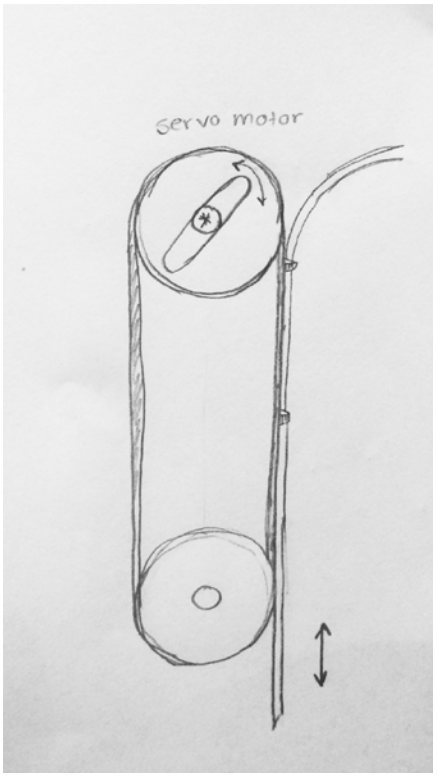

Figure 17: Conceptual drawing of the pulley design.

Slide Potentiometer

Taking all of these options into account, the linear actuator was effectively the most ideal option, save for the high cost and bulkiness. We opted to find a lightweight, inexpensive version of this device and encountered the motorized slide potentiometer (slide pot). This option was smaller, relatively lightweight, fast, very reasonably priced, and capable of position sensing, which is crucial to our design. Since this discovery proved to be very promising, we pursued it further. Shown below is an image of this product.

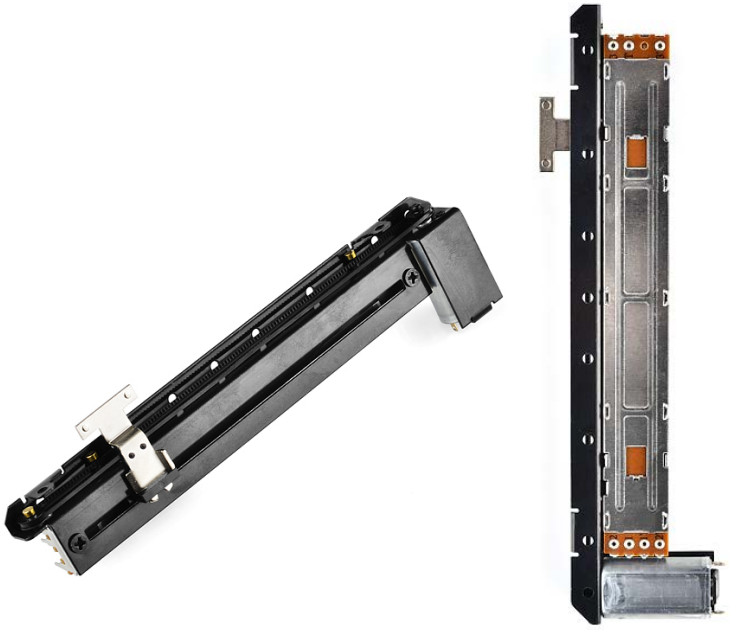

Figure 18: Slide potentiometer from Sparkfun Electronics.

In order to optimize our design, we had to consider the specifications for each design we conceptualized. The specific factors we considered included range of motion, relative accuracy, speed, cost, control system, and which motor is included in the design. We estimated range of motion based on information provided by motor data sheets or through calculations, if the motor would be incorporated in a system we developed. Accuracy was qualitatively approximated

based on how we believed the system would perform the required tasks. The speed was evaluated using data sheets; for systems that would have required us to build a motor, we did not include a speed value, as we did not know the specific dimensions of the system. The cost of each system was approximated based on the motor and additional materials required. The control system and motor categories were both dictated by the type of motor being implemented. A summary of each of these specifications can be found below in Table 3. Prior to conducting these experiments, we will prioritize our design choice based on the holistic optimization of specifications, including the relative qualitative characteristics.

Table 3: Design Specifications to Facilitate Optimization

Z-axis Movement (50mm)	**Linear Actuator[1]**	**Pulley**	**Screw**	**Platform[2]**	**Rotating Tire**	**4-Link Hinge**	**Slide Pot**
Range of motion	10-100 mm	100 mm	100 mm	100 mm	100 mm	100 mm	100 mm
Accuracy	High	Medium-High	Medium	Medium	Medium	Low-Medium	Medium
Speed	23 mm/s	123 mm/s	<100 mm/s	<100 mm/s	123 mm/s	123 mm/s	200 mm/s
Cost	$70-90	~$30	~$30	~$75	~$30	~$30	$19.95
Control system	Direct position	Direct position	Direct position	Direct position	Direct position	Direct position	Motor speed control
Motor	Internal stepper	Servo[3] (13.6g)	Stepper[4] (200g)	Stepper/ High torque servo[5]	Servo	Servo	DC

[1] http://www.firgelliauto.com/products/high-speed-actuator
[2] http://www.ctechglass.com/ctech-lj2503-p-47.html
[3] http://www.rakuten.com/prod/neewer-mg90s-metal-gear-rc-speed-torque-micro-servo-9g-for-trex-align/275316982.html?listingId=375596357&sclid=pla_google_NeewerDirect&adid=29963&gclid=CIS38sH2z8ICFchr7AodCkIAtg
[4] http://www.adafruit.com/products/324?gclid=CNz7rez3z8ICFcXm7AodgH8A9g
[5] http://www.gpdealera.com/cgi-bin/wgainf100p.pgm?I=FUTM0654

4.3 Functions (Specifications)

After constructing the chosen design, we will conduct validation tests to make sure that the design is properly fulfilling each constraint specified by our advisor. Table 4 below outlines these tests. In order to quantify chemical crossover, we will fill each well with water in place of a chemical, and we will use spectroscopy, which is a method of determining the concentration of a substance present in solution by measure the way light is absorbed or reflected through the liquid, a pH test after dissolving a solute in each well (for example, salt), or gas chromatography, which is a way to determine the chemical purity of a solution. To sense pressure feedback when the tube is inserted into the well, in order to make sure the tubing does not hit the bottom of the plate, we can either place a very sensitive pressure sensor underneath the plate and have a continuous reading of the pressure available, or we can monitor the feedback from an actuator attached to the tubing. To ensure proper flow rate, trial and error is an option, in which we will adjust the height of the 96-well plate to approximately adjust the flow rate. We can also calculate the flow rate across the arena, since it is constant, using the volume of the liquid and the distance across the arena. Additionally, we could calculate the flow rate through the tubing using the height of the column and the density of the liquid. Lastly, to ensure proper speed of chemical extraction, we can record the change in height over time using imaging software, or we can attach a marker at a certain position on the tubing and use visual confirmation that it is moving at an appropriate speed.

Table 4: Function-Means (Morphological) Chart for Validation Tests

Function	Means		
	1	**2**	**3**
Quantify chemical crossover	Spectroscopy	pH test	Gas chromatography
Sense pressure feedback	Pressure sensor under plate	Feedback from tubing actuator	•••••
Ensuring proper flow rate	Trial and error	Calculate flow rate across arena	Height and density calculation
Ensure proper speed	Record and analyze change in height over time	Visual confirmation of flow through tubing	•••••

4.4 Feasibility Study/Experiments

To assess the feasibility of the developed system, there are a number of studies that must be conducted. These experiments range from those that ensure the fundamental design objectives and constraints are met, to those that determine the system's ability to successfully reproduce *C. elegans* chemical screening assays. These procedures were introduced in Section 4.4, but we will go into greater detail about our experimental protocols in this section.

To prove that our design is a feasible solution to the problem being addressed by this research, there are a number of explicit benchmarks that must be assessed. These milestones include the quantification of chemical crossover, the determination of pressure feedback, the establishment of proper flow rate, and the verification of timely switches between chemicals. To analyze these parameters, we will evaluate the means presented above in Table 4.

To quantify the rate of chemical crossover, we will use either spectroscopy or a pH test. We anticipate that these means will be reliable and provide a timely and cost-effective way to assess our system. Both of these means involve similar experimental protocols; we will load a 96-well plate with either a dye of known concentration or a salt solution of known pH. These solutions will represent the "chemical" being studied for level of crossover. The first column of

the well plate will alternate between “chemical” and distilled (DI) water, and the second column will be filled with the same stock of DI-water used in column one. With this protocol, we should be able to measure the level of dye carried from the first “chemical” well to the second, after it has been rinsed. This will be determined using spectroscopy to measure the concentration of dye in the second well (which should be just DI-water) after the tubing has been moved to it, or by determining the pH of the liquid in this well.

As discussed in the previous section, we will measure the degree of contact between the tubing and the bottom of the 96-well plate using either a sensitive pressure sensor or by direct feedback from an actuator. This evaluation will depend on which final design we choose to implement for the z-axis movement. If we use one of the design options that utilizes a servo motor, we will likely have to use the pressure sensor, as the motor will likely not have feedback capabilities. Some of the linear actuators we have researched include a feature for feedback, therefore if we choose to implement on of these motors, we may not need an external pressure sensor to conduct this preliminary measurement.

Our assessment of flow rate through the microfluidic arena will be mathematically evaluated and confirmed with trial-and-error experimentation. We will utilize all three of our means for this research, beginning with a mathematical calculation of flow rate, followed by a measurement of the flow rate across the arena, and finally by observing the amount of liquid that passes through the system over a specific duration of time. To measure the flow rate across the arena, we will pulse dye through the microfluidic arena and quantify the time it takes to pass from one side to the other. In a similar manner, we will flow liquid through the system for a specific duration of time (e.g. 1-10 minutes) and measure the volume that accumulates in the outflow reservoir. This final step will allow us to adjust the height difference of the inflow and

outflow locations to optimize the flow rate of the system (i.e. 0.01 mL/min). Our preliminary studies will also involve testing the flow rate when the system is operating under experimental conditions. These tests will include determining the duration each well can be drawn from and confirming that the flow rate remains constant after each chemical switch.

Our final preliminary study will be to evaluate the speed of chemical switches. This parameter has been thoroughly investigated in our search of an optimal z-axis component for the automated system. Once this component is incorporated, we will quantify the rate at which the movement from one well to the next occurs, by recording the switch and analyzing the video. This will also be studied by determining the rate at which one "chemical" clears the arena and is replaced by another. This will likely be conducted by alternating a clear liquid (i.e. S. basal buffer) with a buffer containing dye.

Upon completion of the preliminary studies used to ensure that all of design constraints are met, we will conduct experimental studies using *C. elegans*. The initial experiments will involve repeating a chemical screening assay that has been previously studied using the manual method. This comparison will allow us to assess our system's ability to reproduce scientific data, which is needed to draw the conclusion that it is a successful alternative to the manual method, which is the current gold standard. We will likely reproduce a small-scale version of the AWA chemical screen presented by Larsch et al., in which neural responses to a range of chemical molecules were assessed by quantifying change in fluorescent intensity.

4.5 Modeling

In order to test the validity of our designs we created SolidWorks models. The current system was assembled using parts from OpenBuilds online resource center, such as the gantry V-slot plate, the V slot bars, wheels, and screws seen in Figure 19. The initial automated system,

built by our advisor, was responsible for x- and y-axis movement. Our project addresses the z-axis movement and creates a platform to hold a 96-well plate during testing. The modeling system is used to test the physical constraints and barriers surrounding the platform and z-axis design components.

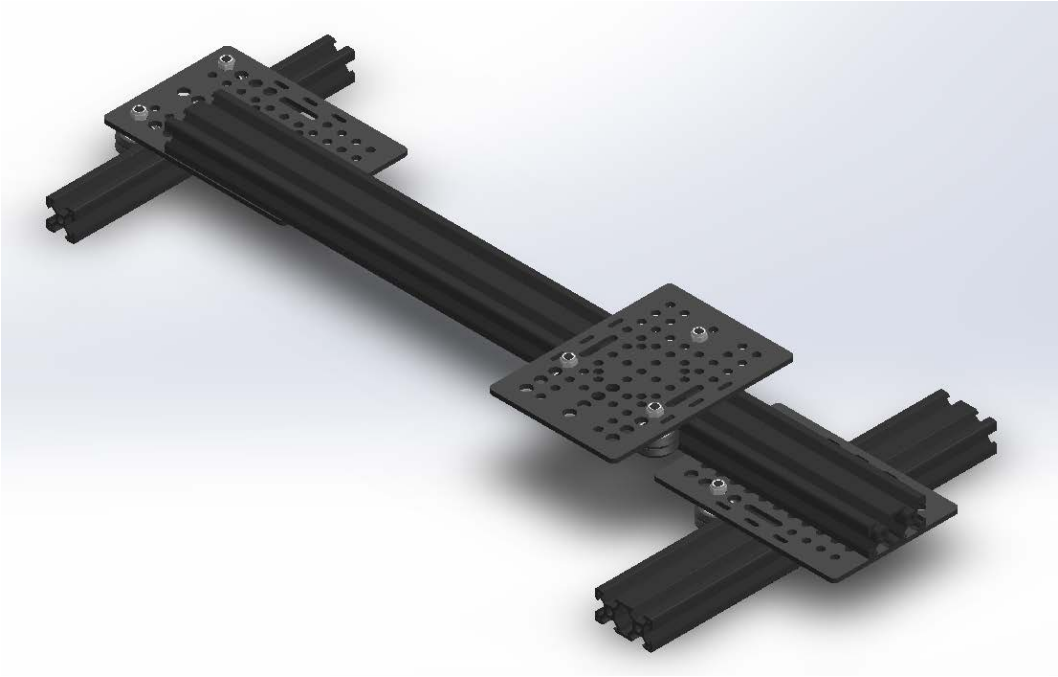

Figure 19: Current automated system, responsible for x and y axis movement, in Solidworks

In SolidWorks, we were able to accurately model the size and dimensions of the 96-well plate platform, shown below in Figure 20. This model will be 3-D printed and attached to the current system to determine if there are any spacial constraints that SolidWorks did not display. Figure 21 displays the 3-D printed platform integrated with the system.

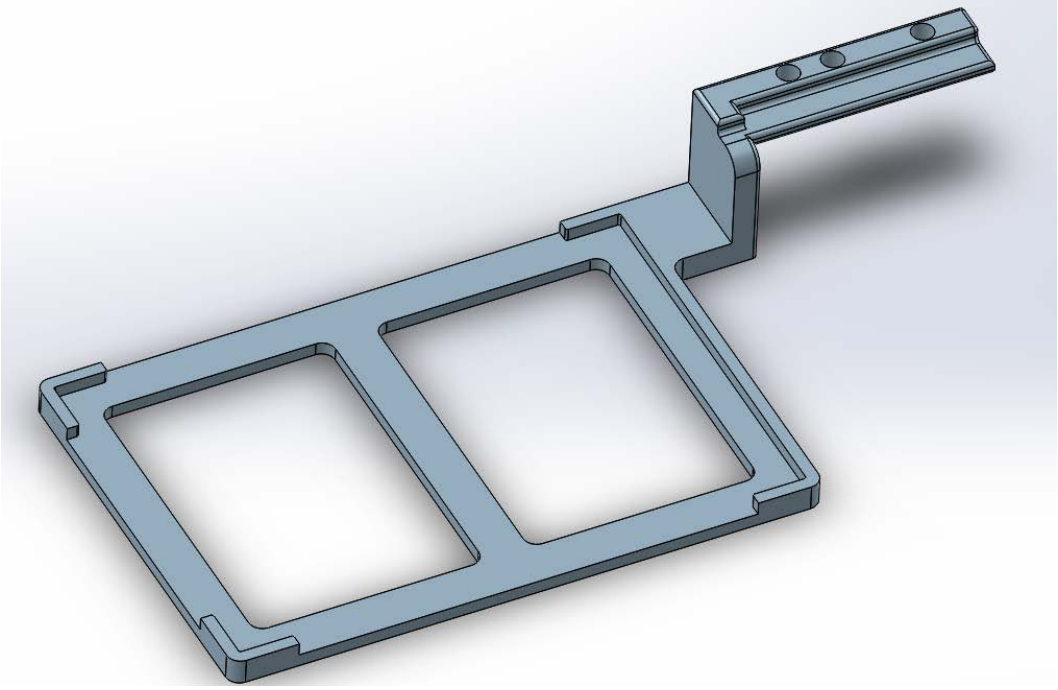

Figure 20: 96-well plate platform model for 3-D printing

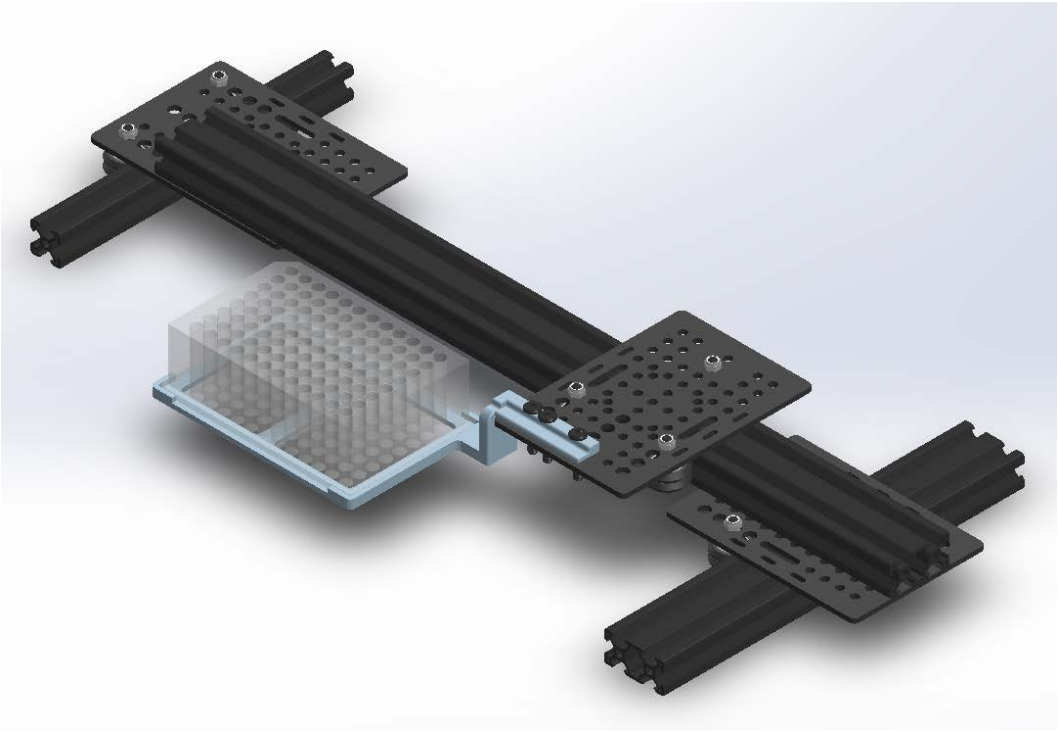

Figure 21: 3-D printed platform model with 96-well plate and current x- and y-axis system

To assess the preliminary SolidWorks design of the 96-well plate platform with the current apparatus, the model 3-D printed in Worcester Polytechnic Institute's rapid prototyping lab is shown in Figure 22. The printed model was then screwed and secured in to the designated V-slot plate.

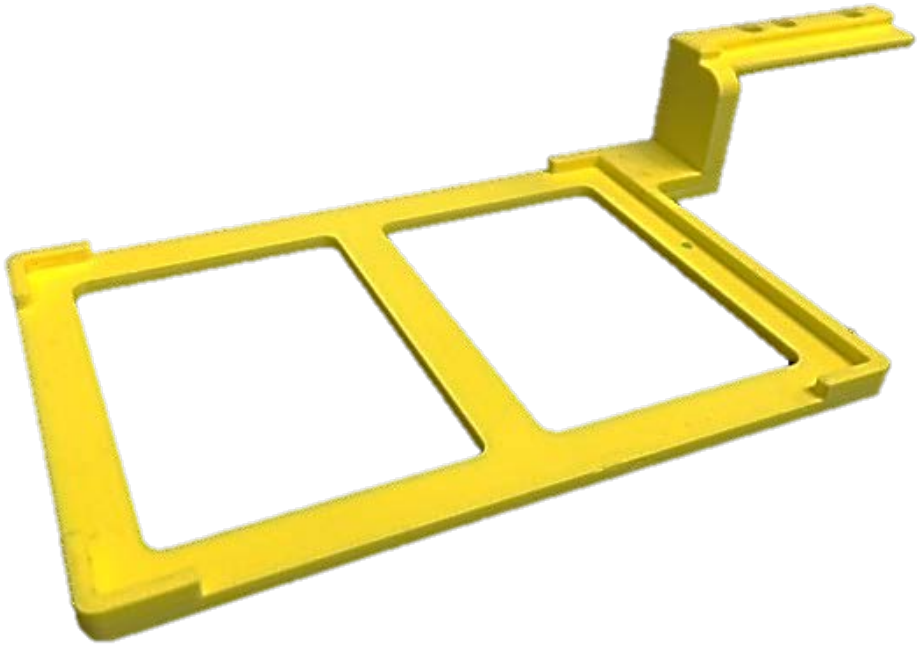

Figure 22: Preliminary 3-D printed platform

After testing the 3-D printed model with our current system, we will machine the finalized platform from compressed aluminum. In order to machine this platform, it needs to be split into two components to conserve material and minimize cost. The two components include the arm and the base seen in Figure 23.

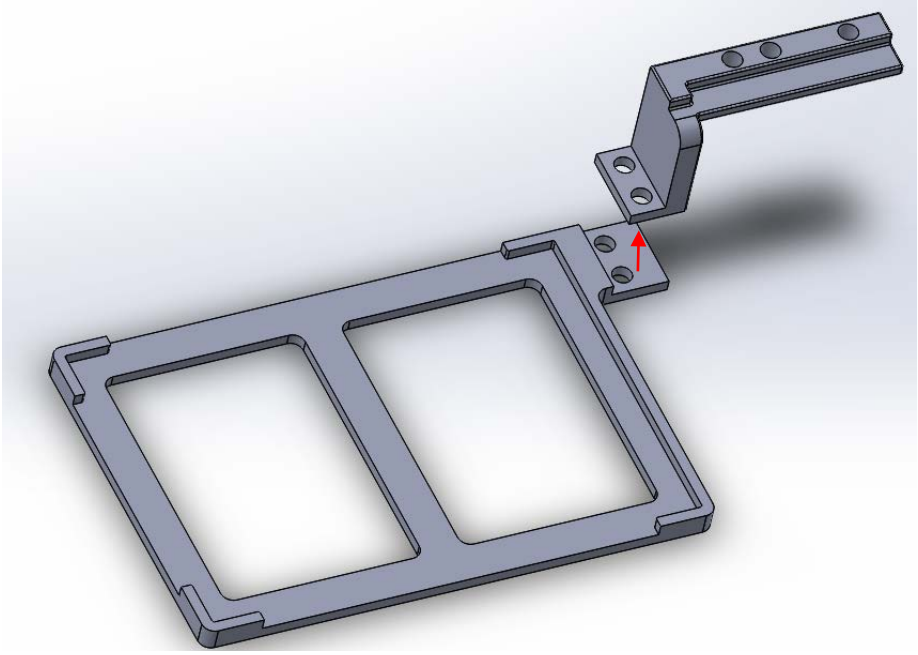

Figure 23: The base and arm of the platform model that will be machined as the final product

Before machining the base and arm of the platform, we evaluated the 3-D printed model and created another model of the machined part with the current system (base-teal, arm-gray), shown below in Figure 24.

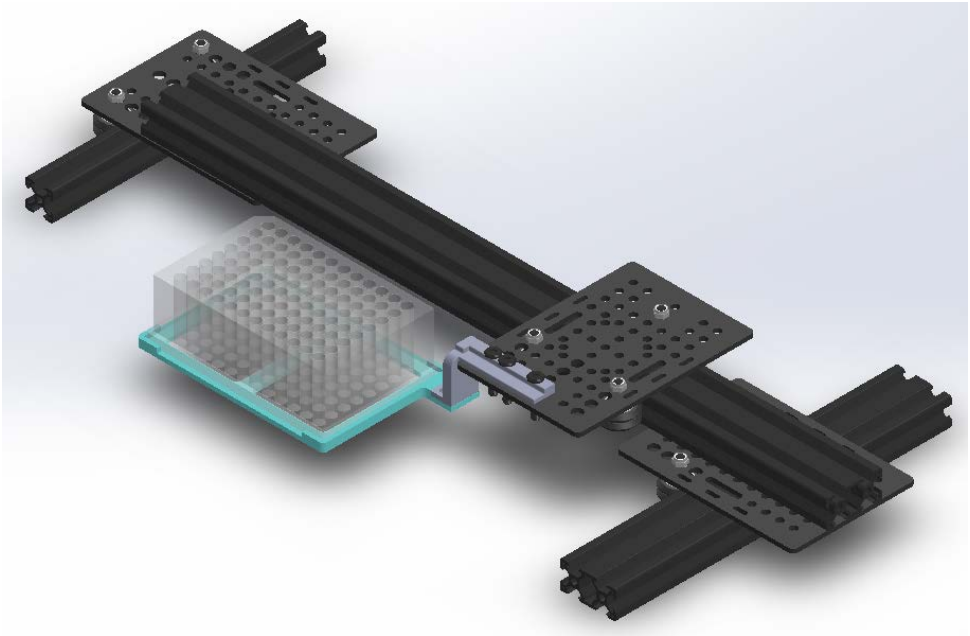

Figure 24: Machined base and arm model with the x and y system

4.6 Preliminary Data

4.6.1 Load Test from SolidWorks

Upon integrating the preliminary 3-D printed platform with the current apparatus, the platform deformed under the weight of the 2ml 96-well plate. This deformation caused the platform to collide into various parts of the imaging apparatus. A new design was created as a solution to the deformation. The base of the plate was made 2mm thicker (from 3mm to 5mm), a taller wall was inserted along the back of the platform (height of 7.5mm) to prevent medial bending, and the arm was thickened to absorb more of the stress applied by the force. The stresses of the new design can be seen below in Figure 25. The dimensions for this platform can be seen in Appendix D.

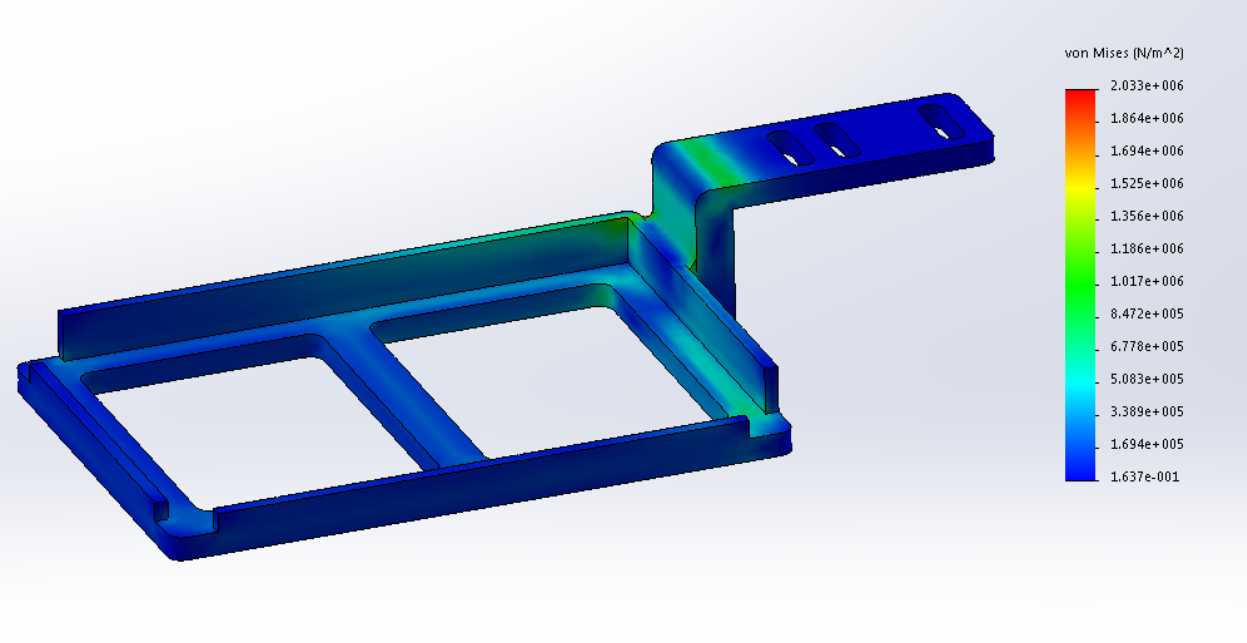

Figure 25: Stress Present of Updated 96-Well Plate Holder Design

Figure 26 below displays the newly rendered platform with ABS plastic material, under a force of two Newtons. The scale bar to the right of the platform displays the location of

maximum displacement the platform will experience under a 2N load. The maximum displacement ~ 1.1mm is shown in the far corner of the platform. Since the displacement does not exceed 1.1 mm, the platform will not collide with the imaging apparatus.

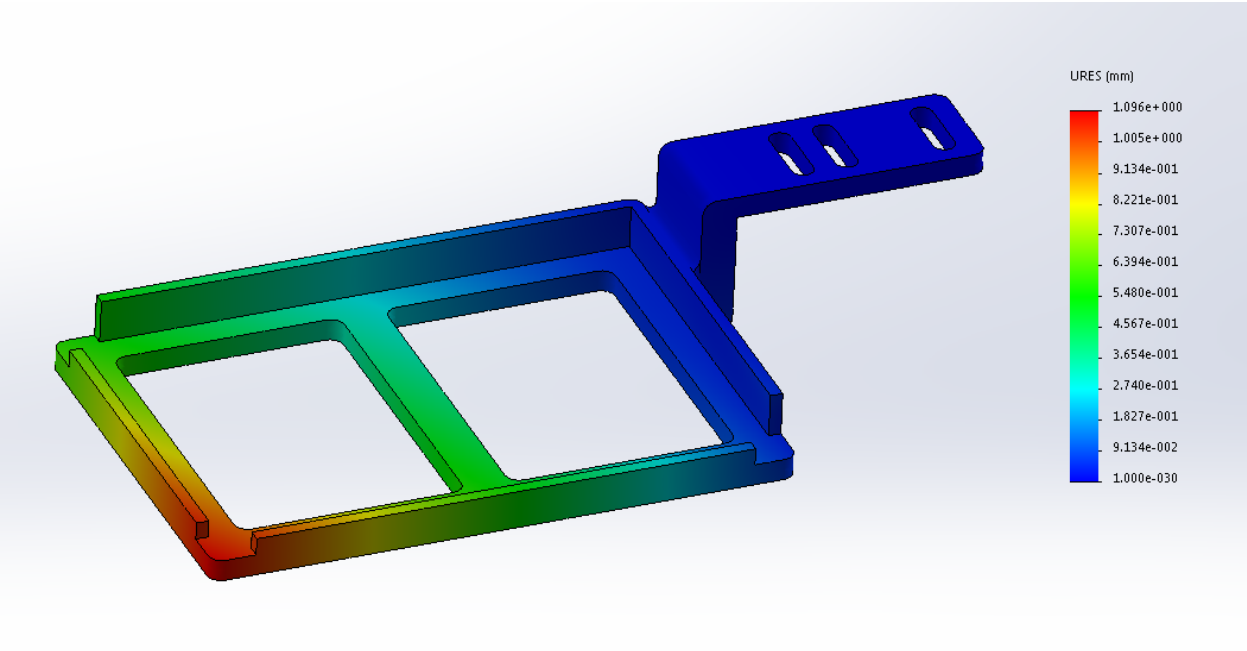

Figure 26: Displacement of the Updated Platform made of ABS under the Force of 2N

After this modeling, we went ahead and 3-D printed the holder once again. The final product can be seen below in Figure 27.

Figure 27: Updated 96-well Plate Holder 3-D Printed

4.6.2 Arduino and Slide Potentiometer

To test the speed and strength of the slide pot, we first connected a 9 volt battery to its terminals and switched the polarization of the battery back and forth to qualitatively observe how fast the slider moved from one extreme of the track to the other extreme. We determined the speed was adequate, so we proceeded to crudely test the strength by suspending the slide pot, with a sharpened piece of tubing attached to the slider, above a 96-well plate covered with plastic seal, and switching the terminals of the battery so that the slider would shoot downwards and the tubing would pierce the seal. The outcome was satisfactory, as the seal was pierced almost every try, so we continued to test the speed and strength of the slide pot more accurately, using Arduino software and hardware.

Initially, we tested the integration of the slide pot with Arduino software and hardware by connecting it to the Uno microcontroller board. This test performed the same motion as our first test, shooting from one extreme of the track to the other extreme. Refer to Appendix A for the sketch containing the code used for this test.

Per our advisor's suggestion, we used the position sensing functionality of the potentiometer on the slide pot. This facilitated the accuracy of its movement when we implemented Arduino code to control it. Each position on the track of the slide pot was assigned a number 0 through 1023. Our goal was to move the slider from position 0 to roughly position 400 as quickly and precisely as possible, stay at that position for several seconds (however long it takes the x-axis and y-axis movements to complete), and then move from position 400 to position 0 as quickly and precisely as possible, without overshooting or ricocheting backwards at any point throughout this process. Since we had already tested that the slide pot was strong and fast enough, we wanted to make sure it could reach those same criteria while traveling a smaller distance both ways; after adjusting parameters such as the position of the origin and the speed, this result was satisfactory. Refer to Appendix B for the sketch containing the code for this test.

Also per our advisor's suggestion, we used the Arduino Motor Shield Rev3 to facilitate the controls of the slide pot's DC motor. This motor shield is based off of the L298, which is a dual full bridge driver that takes transistor-transistor logic levels as an input, and in turn "drives inductive loads such as relays, solenoids, DC and stepping motors" (L298 Dual Full Bridge Driver). The motor shield independently controls each attached motor's speed and direction, and it can control two DC motors, or one stepper motor.

After conducting simple tests using a digital multimeter to measure the voltage passing through the motor shield and confirm that it is compatible with the voltage levels passing through the setup, we combined all of our z-axis components with our advisor's previous work, so that the slide pot could run off of the same Arduino Uno that controlled the x- and y-axis system. Following this, we combined the code that controlled the x- and y- axis system with our code as well.

After combining the components together, we realized powering the slide pot with household electricity, versus a 9 volt battery, resulted in very fast and powerful movement, to the point where we needed to reduce both, or at least find a way to buffer the slide pot's movement. We attempted this by changing the parameters of the code once more, creating a buffer in the code, and creating a small physical buffer at the bottom of the slide pot as well. Ultimately, our code setup included a function in which the slider would slow down as it approached its destination. Refer to Appendix C for the sketch containing the code used for the entire apparatus.

Once we determined our integration of each component to be satisfactory, we focused on combining the Arduino code of the x-, y-, and z-axis components with the software controlling the microscope, Micro-Manager. When the Arduino-controlled system's movement completes, it sends a signal to Micro-Manager, which streamlines the timing of each movement.

4.6.3 Z-Axis Mounting

After coordinating the x-, y-, and z-axis movement came the task of mounting the z-axis component and connecting the tubing to it. As a preliminary test, the slide potentiometer was secured to a ring stand and the rigid tubing was attached to the moving part of the slide potentiometer using tape. Once the principles behind that test were confirmed, a more permanent mounting solution needed to be established.

To suspend the device an appropriate distance above the 96-well plate, an apparatus consisting of three stainless steel bars was constructed. The bars were secured together with cross bar holders and then attached to the entire imaging apparatus, as seen in Figure 28 below. The cross bar holders are adjustable so that the height of the horizontal bar can be changed. The bars were also sawed to a shorter length so as not to protrude unnecessarily.

The slide pot has two mounting holes in it, two centimeters apart from each other, so that it could be secured to another device. A piece of sheet metal was acquired and cut into a triangle, in which we drilled three holes, two small ones, two centimeters apart and one large one, so that it would secure the potentiometer and be connected to the mounting bars. To incorporate the slide pot for z-axis movement, we connected the slide pot to the aluminum triangle, and the aluminum triangle to the horizontal mounting rod, securing it over the 96-well plate, as shown in Figure 28 below. We connected the slide pot to two of the holes we drilled at the vertices of the triangle, using nuts and bolts of sufficient size for fixation. The third vertex was connected to a small mounting rod, which was fixed with another cross bar holder. We were able to change the specific location of the slide pot by adjusting the position of each mounting rod with respect to the cross bar holder.

After that was accomplished, the tubing needed to be attached to the potentiometer. To make sure that the rigid tubing would not bend upon contact with the plastic seal, it was decided that placing the tubing into metal hypodermic tubing would ensure that no bending would occur. The hypodermic tubing would also be able to be permanently mounted to the slide pot and the tubing would easily be changeable. The hypodermic tubing was selected to make for a secure fit and was long enough to make sure the tubing could hit the bottom of the well with no detrimental bending of the tubing. Upon choosing the best fitting hypodermic tubing, which was 2 inches in length and has an inner diameter of 0.061 inches, a portion was carved out using a Dremel tool so that the tubing could be inserted in the middle of the tubing so as to minimize the length it took to reach the microfluidic arena. It was then secured to the moving part of the slide pot using malleable wiring. The entire setup can be seen below in Figure 28.

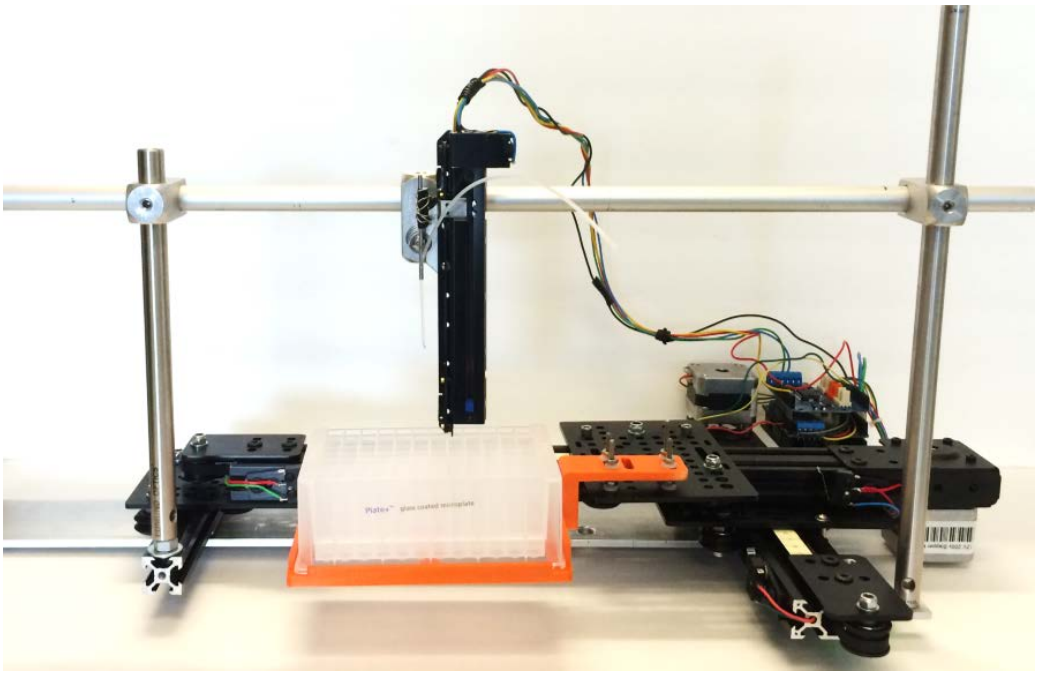

Figure 28: Slide pot and rigid tubing mounting setup

4.6.4 Initial Dye Test

To assess the functionality of our assembled automated system, we conducted an initial dye test. This experiment involved executing a series of well switches, alternating between dyed water and clean water. The purpose of this study was primarily to confirm the ability of our system to work given a set of sequential commands. Our plan was to flow dye from well A1 through the microfluidic system, then to stop the flow, switch to well B1 to rinse, and continue on to well A2, which contained pure water. This simple test would allow us to evaluate a number of preliminary success parameters qualitatively. Firstly, we wanted to make sure that liquid would flow from the 96-well plate to the arena. Secondly, we wanted to ensure that air bubbles were not introduced during the switches. Lastly, we wanted to see, in general, how much residual dye was left over after the rinse cycle.

For this study, we used a microfluidic device created by our advisor, which is named "P2". This device (shown below in Figure 29) has four inlets, one worm loading port, and one outflow port. In the figure, “A” denotes the buffer port, “B” denotes the chemical inlet, the control inlets are abbreviated “ctrl1” and “ctrl2”, “loading” indicates the worm loading port, and “out” refers to the outflow port.

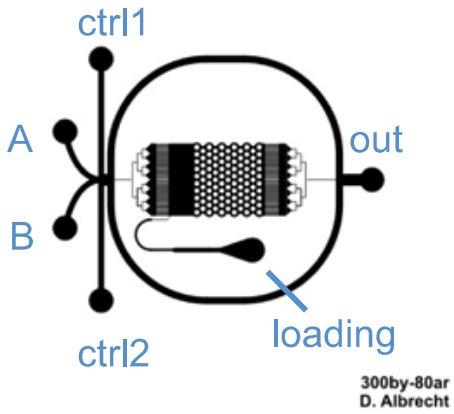

Figure 29: P2 Microfluidic Device

Usually, the four inlets are used to connect the chemical-containing reservoir (i.e. 96-well plate), a buffer reservoir, and two tubes that are attached to a control reservoir via a switch valve. The only liquids that ever flow through the arena are the chemical and the buffer. Only one of these liquids ever flows through the arena at any given time, and their alternation is dictated by whichever control liquid is flowing. For simplicity, we used a P2 device that only had the chemical and buffer inlets punched. With this setup, we could not switch between the two liquids, as they both flowed through the arena at the same time, but it was very simple to balance the flows of the two inlet liquids, which allowed us to determine an appropriate mounting height for the buffer reservoir. For the purpose of qualitatively evaluating functionality of our system, this two-inlet P2 device was suitable.

Unfortunately, we ran into an obstacle during the first step of this evaluation—when we set up the system and began to flow the dye, it did not enter the arena. We deduced that this was due to the fact that the accompanying buffer reservoir experienced less resistance than the well containing dye. We further realized that this was likely influenced by two factors, the height difference of each reservoir (i.e. buffer and well) and the length of each tube connecting the reservoirs to the arena. Once we balanced the heights to compensate for the variation, we were able to visualize the correct distribution of the dye and clear liquid in the arena. Due to some bubble complications, unrelated to the automated switching, we were not able to assess whether the act of switching would introduce bubbles. Additionally, because the dye was very faint, we were not able to quantify how much residual dye was left after each switch. Due to these obstacles, we planned a series of validation experiments that would allow us to qualitatively and quantitatively evaluate these parameters.

Chapter 5: Design Verification & Results

We conducted three main validation tests, including a switching rate study using fluorescein, a cross-contamination study also using fluorescein, and a neural screening assay with *C. elegans*, using the attractive odor diacetyl. These experiments were both progressions from the initial dye test, since the results from that validation test were not conclusive, nor did they provide us with quantitative results. Overall, the purpose of these tests was to validate that our initial constraints and objectives were met.

5.1 Chemical Switching Rate

We initially tested the duration needed to completely switch from fluorescein to DI-water. To do this, we established the flow from a fluorescein-containing well, and switched the tubing to a DI-water well. We recorded this transition using fluorescence microscopy, and quantified the results of this transition using an ImageJ tool that analyzes fluorescent intensity levels over time, called “Intensity vs Time plot”. The results from this analysis are shown below, in Figure 30. When the fluorescence levels out at the baseline intensity, this signifies a complete chemical switch, which occurred after approximately 50 seconds.

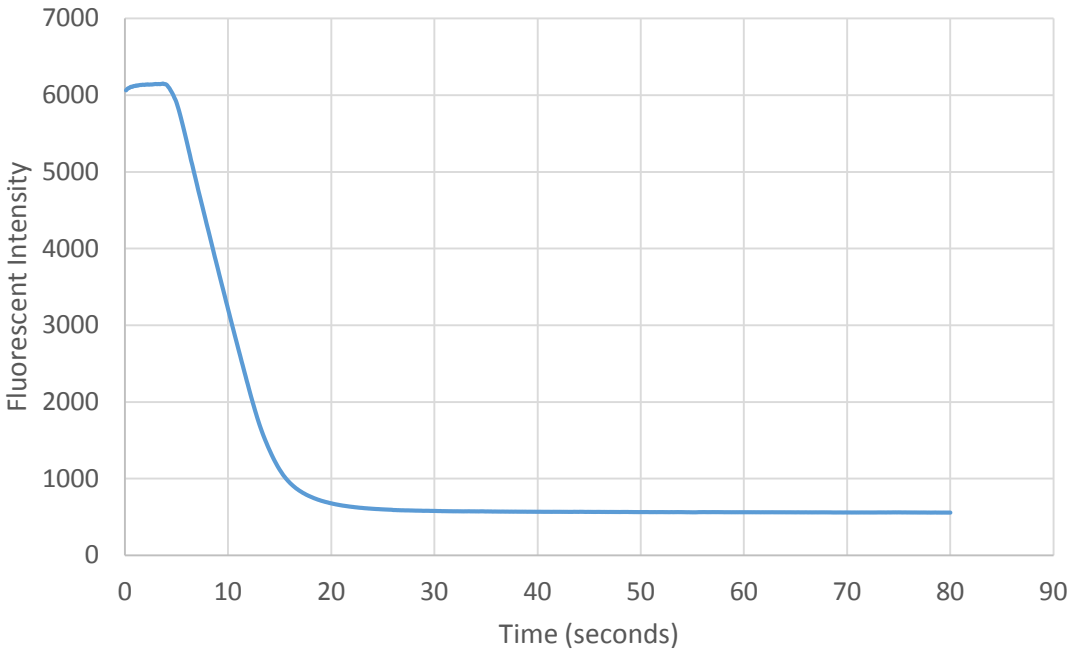

Figure 30: Chemical switching rate using fluorescein and ImageJ to quantify results

5.2 Cross-Contamination Study

As previously discussed, one of our experimental constraints included having a chemical carryover less than 0.01%. We tested this value by using fluorescein and water as substitutes for the chemicals that would be used in a traditional chemical screening experiment. The reason we used fluorescein and water was because they provided us with a useful platform to assess cross-contamination between chemicals quantitatively. Fluorescein is a molecule that fluoresces when exposed to blue fluorescent light, thus it is very useful as a tracer for imaging. This validation test was conducted using two distinct experimental methodologies (i.e. without and with a rinse), as shown below in Figure 31 and Figure 32, respectively. For our experiments, we conducted method one using wells A1-A12, and method two using wells A1-A6. During the study of Method 2, air bubbles entered the microfluidic arena during the latter portion of flow from the

well-plate. For this reason, to maintain consistency for our results, we performed a cross-contamination analysis of only wells A1-A5 for both methods.

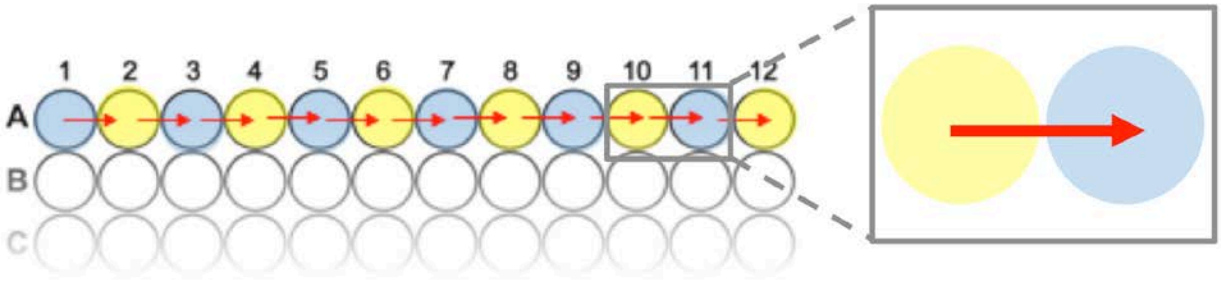

Figure 31: Method 1 for fluorescein cross-contamination, without rinse between switches

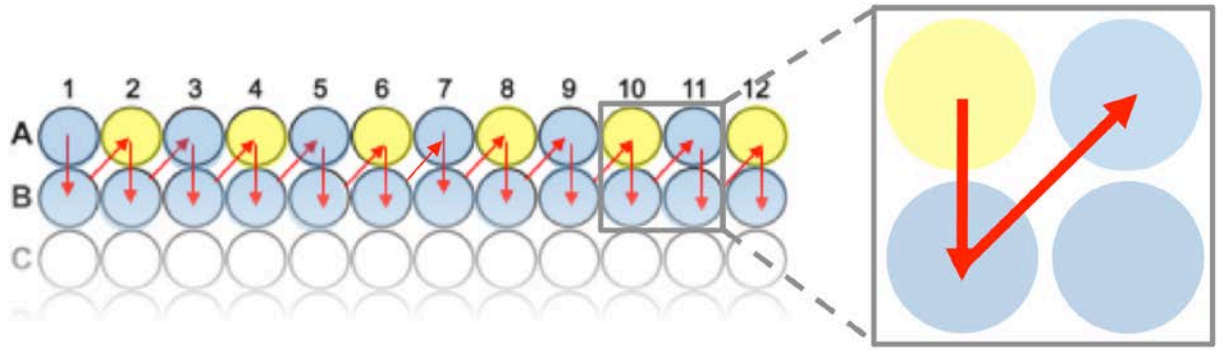

Figure 32: Method 2 for fluorescein cross-contamination, with rinse between switches

We used the ImageJ tool previously discussed to evaluate the amount of cross-contamination present during the switches from each fluorescein containing well to the successive water well. The analysis process began by establishing a baseline of fluorescent intensity, which was done using well A1, as it contained pure DI-water. The analysis for this baseline well is shown below in Figure 33. Two measurements of fluorescent intensity were taken for each set of images, one in the experimental area of the microfluidic arena, and another in a background region of the PDMS where no liquid was present throughout the experiment. By taking two separate measurements, we were able to compare the intensity levels, per frame, reducing the noise that may be present due to fluorescein's sheer intensity affecting the areas that

did not contain the compound (i.e. the background PDMS). To quantify cross-contamination between wells, we took measurements of fluorescent intensity from the wells that contained fluorescein, and we compared these values to the succeeding water wells that ideally do not contain any fluorescein, unless contaminated.

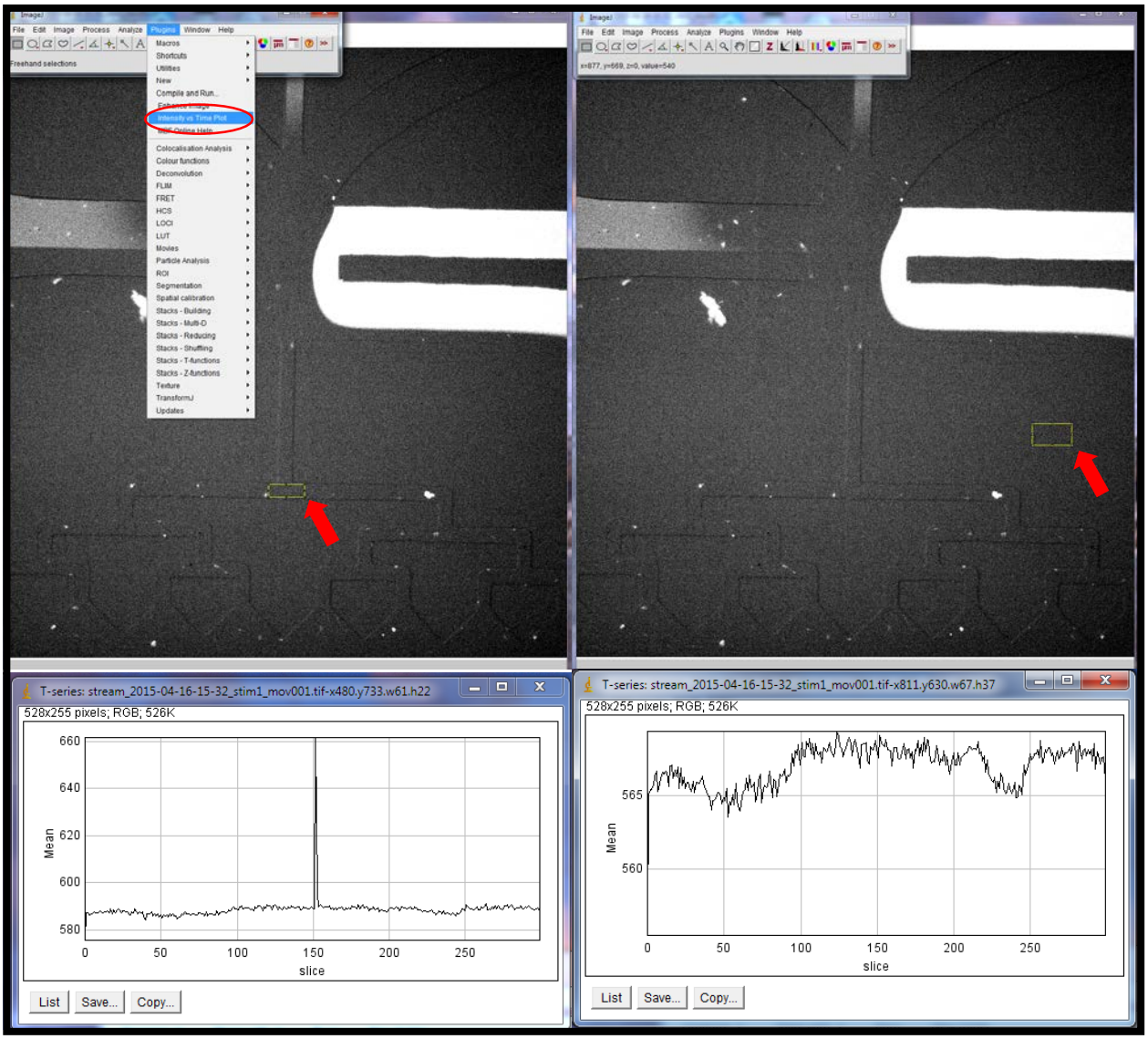

Figure 33: Image J software that was used to analyze the fluorescent intensity of the DI-water entering the microfluidic arena. The yellow box (indicated with red arrow) is the area that is being analyzed. The graphs display the change in mean fluorescent intensity over time (slice of image).

Figure 34 below shows the microfluidic arena during flow from a fluorescein experimental well (well A2). The fluorescein wells elicited a spike in intensity over time until the

stimulus was removed. The background PDMS measurement in the figure below is used to quantify how much the fluorescein affected the fluorescent intensity of the "background" or surrounding PDMS.

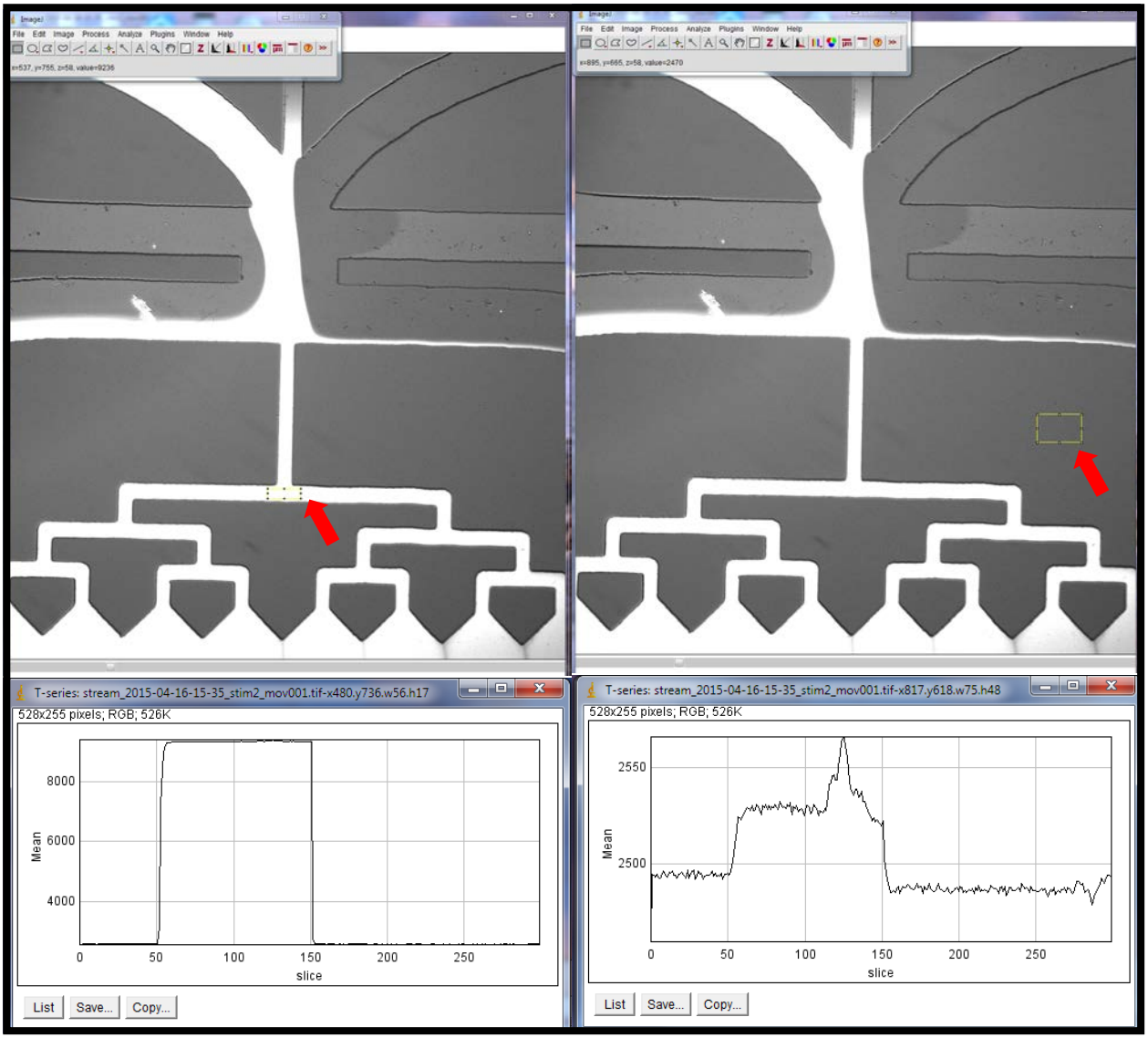

Figure 34: Image J software that was used to analyze the fluorescent intensity of the fluorescein entering the microfluidic arena. The yellow box (indicated with red arrow) is the area that is being analyzed. The graphs display the change in mean fluorescent intensity over time (slice of image).

After we obtained the list of 300 fluorescence data points from each experimental well, which is equivalent to 30 seconds at 10 frames per second, we were able to quantify the results in

Excel using the template shown below in Figure 35. Each 30 second trial included a 10-second pulse of fluorescein, occurring from the 5-15 second marks. By subtracting the background noise from the intensity levels of the experimental region during each fluorescein pulse, we were able to establish a more reliable set of data for each well. The cross-contamination was calculated by analyzing each switch from a fluorescein well to a water well, for example, well A2 to well A3. For this analysis, a comparison was made between the experimental liquid and the control buffer, which, throughout all of our cross-contamination study, was presumably pure DI-water. For our calculations, we used the fluorescent intensity values acquired during the 10-second pulse of fluorescein to quantify cross-contamination. The results from this analysis are shown below in Table 5. It should be noted that in each of these summaries, the time points are referred to in terms of frame number, i.e. the 5-15 second marks are equivalent to frames 50-150.

O20

	A	B	C	D
1	PDMS measurement (Water well)	Experimental Measurment (water well)	Difference (Exp-PDMS)	
2				
3				
4				
5				
6				
7				
8				
9				
10				
11				
12				
13				
14				

E	F	G
PDMS measurement (Fluor. well)	Experimental Measurment (Fluor. well)	Difference (FL.Exp-FL.PDMS)

I	J	K	L	M
Difference measurments	Water well	Delta	Fluor. well	Delta
Measurment 1 to 50	Average 1:50		Average 1:50	
Measurment 50 to 150	Average 50:150	Avg(50:150)-Avg (1:50)	Average 50:150	Avg(50:150)-Avg (1:50)
Measurment 150 to 300	Average 150:300	Avg(150:300)-Avg(50:150)	Average 150:300	Avg(150:300)-Avg(50:150)
		Avg Delta 1		Avg Delta 2
Cross-contamination:				
Water Well	Avg Delta 1			
Fluor. Well	Avg Delta 2			
	Cross-cont	(Avg Delta 1 / Avg Delta 2)*100%		

Figure 35: Excel spreadsheet used as a template for our data analysis. The highlighted values were the most important for our analysis.

Table 5: Results from the chemical cross-contamination from well A1 to A5, experiment 1 with no rinse and experiment 2 with a rinse.

Experiment 1 (no rinse)	Fluorescent Intensity	Cross-contamination (%)
A1 (water)	0.350553	N/A
A2 (fluor.)	3358.147	0.030872
A3 (water)	1.01267	
A4 (fluor.)	3306.056	0.02017
A5 (water)	0.636682	
Average		0.025521
Experiment 2 (rinse)		
A1 (water)	0.5763	N/A
A2 (fluor.)	6457.982	0.007686
A3 (water)	0.45143	
A4 (fluor.)	6160.797	0.007199
A5 (water)	0.505895	
Average		0.007442

The graphs in Figure 36 below display the change of fluorescent intensity per each experimental well, from water wells (A1, A3, A5) to fluorescein wells (A2, A3), using each methodology.

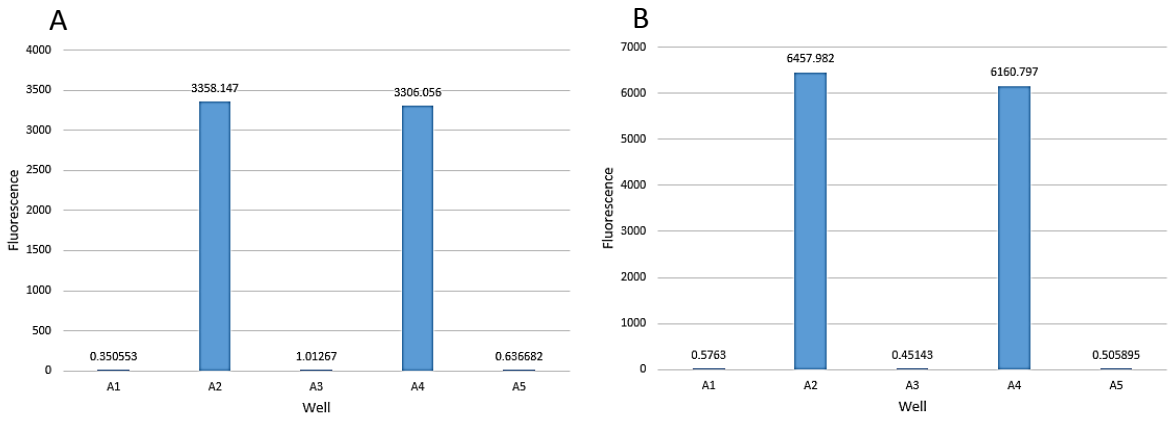

Figure 36: (A) Experiment 1: Fluorescent intensity per each well plate with no rinse; (B) Experiment 2: Fluorescent intensity per each well plate with one rinse.

Through these experiments we found that without a rinse cycle the cross-contamination was 0.0255%. With the inclusion of a rinse cycle during screening experiments the chemical cross-contamination was 0.0074%.

5.3 *C. elegans* Automated Chemical Screen

Once we completed the tests required to validate that our initial objectives and constraints were met, we needed to evaluate our system's ability to replace the manual method for *C. elegans* chemical screening. To do this, we reproduced an experiment that was previously conducted with the manual method, using our automated system, and compared the results obtained from each methodology. The experiment, which was originally conducted by Larsch et al., involved studying the neural response of a worm strain with fluorescently labeled AWA neurons, by means of calcium imaging. This study demonstrated that these neurons respond in an attractive manner when the worms are exposed to diacetyl. Furthermore, this study revealed that the calcium response to diacetyl occurred with dose dependency; higher concentrations of diacetyl elicited larger increases in fluorescent intensity levels. The experiment reported in their paper compared a number of different concentrations of diacetyl (i.e. 0.001 μM, 0.01 μM, 0.1 μM, 1 μM, 10 μM, and 100 μM), each of which was exposed to the worms for a 10-second period of time, with 5-seconds of recording before and after exposure, and a 50-second interval without exposure or recording between pulses.

To recreate this dataset, we conducted an automated version, and exposed the worms to six different concentrations, 0.1 μM, 1 μM, 10 μM, 100 μM, 1,000 μM, and 10,000 μM each in triplicate. These diacetyl concentrations were loaded into wells A1, A3, A5, A7, A9, and A11, with intermittent S. basal rinses between those experimental wells. We were able to use all 12

wells for this study, as we resolved the issues with air bubble infiltration that occurred during the cross-contamination tests.

Although we recorded all six concentration responses, including those to 1,000 μM and 10,000 μM diacetyl, Larsch et al. did not report these two concentration levels, so we omitted them in our comparison. To create these concentrations, we performed a serial dilution, beginning with stock diacetyl (1 M). To create 10,000 μM diacetyl, we pipetted 30 μL of stock diacetyl into 30 mL of S. basal buffer. For each serial dilution, we pipetted 200 μL of the previous concentration into 1800 μL of S. basal (e.g. 200 μL of 10,000 μM + 1800 μL S. basal = 1,000 μM diacetyl). This process was repeated for each dilution down to 0.1 μM diacetyl. The worms were exposed to each concentration for a 10-second period of time, with 5-seconds of recording prior to and 15-seconds following exposure. Each repetition was separated by a 30-second period without recording, and each new concentration was separated by 45-seconds.

Concentrations of diacetyl were sequentially delivered to the worms from low (0.1 μM), to high (10,000 μM). The worms' responses were recorded at 10 frames per second, with a blue fluorescent light pulsation rate of 10 ms, which was dictated by the MicroManager system set up on an accompanying computer. For evaluation purposes, there were 11 animals that we were able to analyze for all concentrations, although the device was originally loaded with 21 worms. These animals, along with their tagged AWA neurons, can be seen below in Figure 37. It should be noted that, while there are 13 green arrows in the figure, two of these worms were omitted because they could not be used for all concentrations. This was due to the fact that, despite these animals being immobilized via paralysis, some of the paralysis effects wore off during the experiment, causing them to go out of frame or collide with one another.

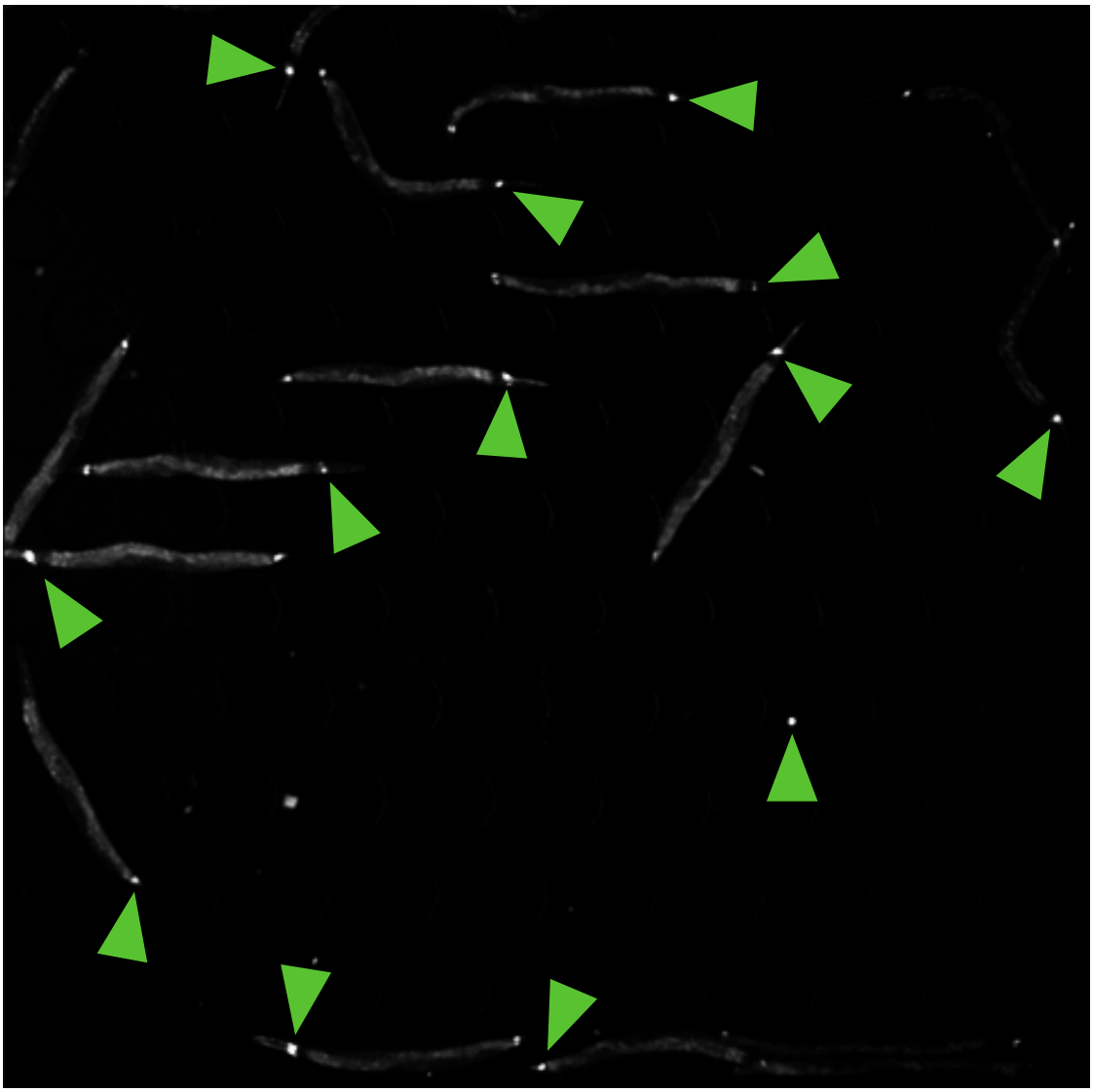

Figure 37: Image of C. elegans' AWA neurons responding to diacetyl, where each animal's AWA neurons are labeled by a green arrow.

Using previously published worm-tracking algorithms (i.e. ImageJ, MATLAB), the fluorescent intensity levels of each worm's AWA neurons were determined with respect to time. These values directly correlate to calcium activity, thus they can be used to measure each worm's neural response. The average neural responses of 11 different worms to each diacetyl concentration are shown below in Figure 38.

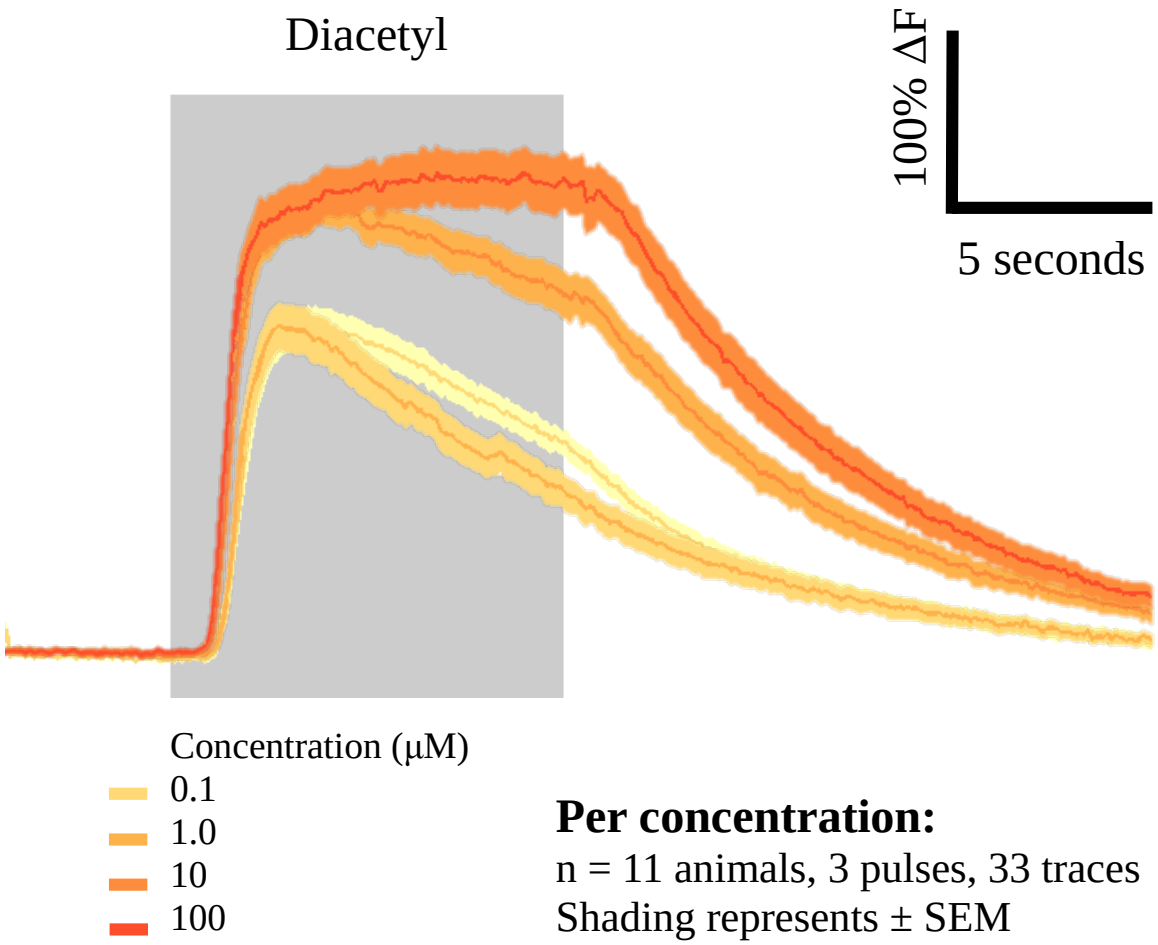

Figure 38: Average dose response of C. elegans' AWA neurons to different concentrations of diacetyl, expressed by changes in fluorescent intensity.

Chapter 6: Discussion

6.1 Our Results and a Comparison to Larsch et al.'s

Our fluorescein study not only confirmed that we could meet our experimental constraint of there being less than 0.01% cross-contamination between chemicals, but it also found a method of conducting this chemical screening experiment that optimizes reaching our cross-contamination constraint, i.e. Method 2 shown above in Figure 32. Therefore, future chemical screening studies would benefit greatly from being conducted using the rinse method.

Our *C. elegans* experimental results align quite closely with those obtained by the Larsch et al. study, which are shown below in Figure 39. The foremost difference between the Larsch et al. methodology and ours is that our study was fully unattended by the researcher due to the aid of our automated system. The Larsch et al. study utilized the manual method described in Section 2.3.1. Additionally, we delivered 10-s pulses of concentrations of diacetyl in triplicate, while Larsch et al. delivered 10 pulses of the same duration. Thus, our complete study was shorter in duration than that of Larsch et al.

Another notable difference between the two studies is that we recorded responses to two concentrations, i.e. 1,000 μM and 10,000 μM diacetyl, and Larsch et al. did not, so we omitted them in our comparison. Additionally, because these concentrations were so high, they caused over-saturated responses in the AWA neurons, thus their inclusion would confound our analysis of the results in comparison to the Larsch et al. study.

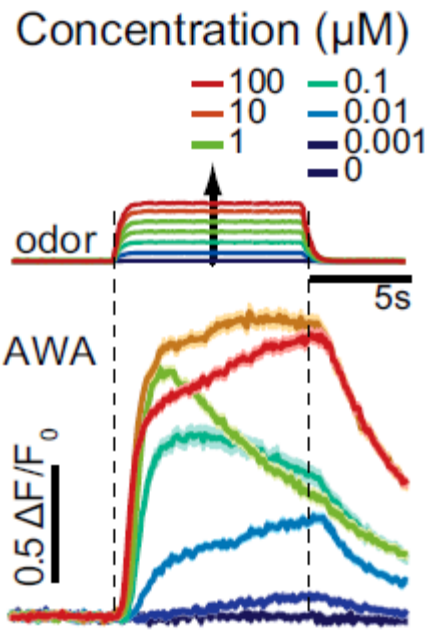

Figure 39: Larsch experimental results; mean AWA fluorescence response to systematic variation in odor concentration (10 repeated 10-s pulses) of diacetyl, n= 40 animals[38]

Since our experimental methodology was very similar to that of the Larsch et al. study, and the results obtained from both were also very similar, we can state that our system was able to correctly conduct a neural chemical screening study in *C. elegans*, without the constant researcher attention and intervention needed for manual chemical screening. There are, however, small discrepancies between our results and the Larsch et al. results, namely the curves for the 0.1μM and the 100μM concentrations of diacetyl. These small discrepancies can possibly be attributed to variation in the worms' AWA neural responsivities, as well as different sample sizes; Larsch et al. studied 40 immobilized animals, while we studied only 11. Additionally, the discrepancies could be attributed to the different number of repeat tests per concentration of diacetyl. Because *C. elegans* can adapt to chemicals, increased exposure to a certain chemical will result in an overall lower dose response. We only delivered three 10-s pulses of diacetyl per concentration, whereas Larsch et al. delivered 10 repeated 10-s pulses to the animals. Thus, the

overall dose responses of the animals in our study are slightly higher than those of the Larsch et al. study.

6.2 Economics

Our system eliminates the need for purchasing the commercial liquid delivery systems discussed above in Section 2.3.2, thus reducing the cost entailing conducting neural chemical screening experiments. The total cost for our system, including the Arduino microprocessors, the aluminum tracks, the aluminum slides, the mounting rods, the slide potentiometer, the rapid prototyped platform, all of the wires, and any other accessories used in the construction of our system, amounted to slightly under $300, which is significantly less expensive of any of the automated systems described in Section 2.3.2, as they were all priced above $10,000. A side-by-side comparison of the cost breakdown in relation to other automated systems is shown below in Table 6.

Table 6: Cost comparison of our system with other automated systems

Part	Cost (USD)	System	Cost (USD)[53]
Tracks, slides, and mounting rods[47,69]	167.00	Biotek Precision Microplate Pipetting System	$20,000
Slide potentiometer	19.95	Biotek MicroFlo	$13,000
Arduino UNO Rev3 microcontroller board[4]	21.16	COPAS BIOSORT	$300,000
Arduino Motor Shield Rev3	21.16	FACS	$18,950
3D printed platform	23.04		
Total cost	252.31		

6.3 Environmental Impact

Our system does not have any significant immediate effect on the environment. Nonetheless, improper disposal of screened compounds can result in chemical pollution, but this

does not have any implications related to our system, as the researcher is responsible for cleaning the work space and proper disposal of experimental compounds.

6.4 Societal Influence

Our system provides a more time-efficient method for neural drug screening studies. If one were to study all 1280 pharmacologically active compounds in the University of Massachusetts Medical School's Small Molecule Screening Facility (UMMS SMSF) library, with three concentrations per compound, it would take 30.27 8-hour work days total, as calculated below in Equation 1 (Parelkar).

Equation 1: Time needed to screen all 1280 pharmacologically active compounds in the UMMS SMSF library

$$4\ rows\ chemical\ wells\ \times 12\ chemical\ wells\ each\ \times 225\ s\ per\ chemical = 10{,}800\ s\ for\ chemicals$$

$$4\ rows\ rinse\ wells\ \times 12\ rinse\ wells\ \times\ 2\ s\ per\ rinse = 96\ s\ for\ rinses$$

$$10{,}800\ s\ for\ chemicals + 96\ s\ for\ rinses = 10{,}896\ s\ per\ well\ plate$$

$$1280\ compounds\ \times 3\ conc.per\ compound = 3840\ chemical\ wells$$

$$\frac{3840\ chemical\ wells}{48\ available\ chemical\ wells\ per\ plate} = \ 80\ well\ plates$$

$$80\ well\ plates\ \times 10{,}896\ s\ per\ well\ plate = 871{,}680\ s = 14{,}528\ \text{min} = 242\ hrs\ \ to\ test\ all\ compounds$$

The times used for individual chemical wells and rinse wells (i.e., 225 s and 2 s respectively), can be altered according to the specific needs for each individual study. Generally, the total duration of a screening study should not exceed several hours, since *C. elegans* responses begin to fluctuate after a certain amount of exposure to neural activity-altering compounds. Thus, as long as the time to screen chemicals using one 96-well plate does not exceed several hours, the individual times for each well can vary. Using our system eliminates the need for constant attention and intervention from the researcher, thus resulting in 242 hours,

as calculated above, that can be dedicated to other tasks, since our system is hands-off and automated. Therefore, our system would save a researcher approximately 30.27 8-hour workdays.

6.5 Political Ramifications

Although our system does not have a direct influence on the culture of other countries, it can increase the pace of worldwide neural research, making access to *in vivo* and clinical trials much easier, thus increasing the chances of finding adequate drug treatments for neuropsychiatric disorders. Building off of these political ramifications of our system, as research in this particular field becomes more prevalent, we feel that mental disorders will become less of a taboo subject in the world, which in turn will fuel neural research even further, thus creating a cycle of acceptance, funding, and research.

6.6 Ethical Concern

Since our system is primarily meant for research using a microscopic, invertebrate animal model, i.e. *C. elegans*, there are very few ethical considerations that must be taken into account. Animal care protocols are used to outline the considerations that must be taken when conducting research using vertebrate models (e.g. mice), but they do not apply to *C. elegans*. There exists a debate over whether or not invertebrates, as a whole, experience pain in the same way vertebrates do. Given that *C. elegans* are invertebrate, low-order organisms, they do not warrant standard animal care practices that are required for higher-order, vertebrate species. While animal testing is a necessary transition between *in vitro* studies and human trials, the use of *C. elegans* is far less unethical than other, more complex animal models.

6.7 Health and Safety Issues

Our system has very obvious and immediate implications in the health and quality of life of those who suffer from neuropsychiatric disorders with no proper treatment options. It greatly increases the possibility of finding drug treatments for mental disorders (such as autism, schizophrenia, depression, and many others), while increasing the potential of minimizing detrimental side effects associated with drug treatments.

As for safety issues in regards to the researcher/user, our system poses very little immediate threat. The slide potentiometer moves very quickly, but the tubing is not sharp or stiff enough to cause personal harm. Contrarily, there is a small risk of a chemical spill occurring, which could potentially damage the objective microscope beneath the microfluidic arena, since it is an electronic device, unprotected from liquid damage. However, this risk is still present during manual chemical screening experiments, although slightly higher with our system, since there is no way for the system to self-correct errors.

6.8 Manufacturability

Our system is very straightforward to reproduce, since all of our materials are open-source. In order to facilitate reproduction of our system, we have included all our schematics and code involved with the creation of our system. Additionally, our system is comparatively more straightforward than other high-throughput screening methods, since highly comparable systems are only accessible via a facility-based approach. A total of 105 laboratory facilities have experimental setups in which microfluidic *C. elegans* screening experiments can be conducted, but the researcher would have to travel to one of the facilities to be able to use it, whereas our system can be assembled and used in any laboratory at a small cost.[1]

6.9 Sustainability

Our system does not have any immediate effect on sustainability, besides electricity usage and the manufacturing of aluminum and rapid prototyped parts. The effects of these factors on the environment as a whole is minimal, thus the production of our system has no significant impact on ecology.

Chapter 7: Final Design and Validation

7.1 Chemical Screening in *C. elegans*

C. elegans are an ideal candidate for chemical screening because of their complete connectome and their genetic conservation to humans, which allows them to model human diseases that can then be tested. These nematodes are ideal for high-throughput testing because they are inexpensive, easily imaged due to being transparent, and are small, allowing many animals to be monitored at once. There currently exists a way to monitor neural responses of *C. elegans* to chemical stimuli and it is high-throughput in that many animals can be monitored at once and that many chemicals can be administered, but it requires the experimenter's presence, which is limiting. Also, timing by an individual experimenter would not be consistent due to human error, so there is a need to automate the process.

7.2 Creating an Automated System for Chemical Screening

The team's goal was to create an automated system that would be able to draw chemicals from a 96-well plate and deliver them to a microfluidic arena where the response of *C. elegans* would be able to be monitored. Using the imaging system already established, the team only needed to be concerned with creating a system that would be able to process input commands that dictate the timing and actions of the system. By creating a system that is able to automate the chemical screening process, the experimenter would save time and the results would be more accurate, due to each stimulus being administered consistently.

7.3 Engineering Design

7.3.1 Overview

The team was given a system with a standard wheel carriage plate that traveled in two dimensions along an aluminum v-rail system. The system was programmed to move in distances that correlated to the length and width of each well in a 96-well plate, so that a vertical component would be able to draw from a specific well when the carriage plate moved. To ensure the proper flow of chemicals, the 96-well plate could not be placed on top of the carriage plate, so as to minimize the height difference of the 96-well plate and the microfluidic arena. The system also had to switch chemicals within 0.5 seconds, which would dictate the speed and range of the components of the system. The team decided to use a system that incorporated a fixed z-axis component, which would draw the chemicals out of the plate, and a movable xy-plane that would facilitate switching between wells.

7.3.2 96-Well Plate Platform

In order for the system to function as desired, the chemical containing 96-well plate needed to be suspended from the x- and y- moving carriage plate so that it was as close to being as low as the microfluidic arena as possible, but while still fitting within the spatial confines of the system already created. Two iterations of a 96-well plate platform holder were constructed in SolidWorks and then 3-D printed. The first iteration showed that the 96-well plate fit within the platform, but was too weak to support the plate without major deformation. The platform was then made thicker with supporting walls to minimize deformation and succeeded at holding the 96-well plate and was firmly attached to the carriage plate.

7.3.3 Slide Potentiometer for Z-Axis Movement

Once the 96-well plate was able to move in the x- and y- direction, a method for moving the tubing in the z-axis to draw chemicals from the wells and deliver them to the microfluidic arena was needed. A slide potentiometer was chosen due to its speed and low cost. The slide pot needed to be programmed using an Arduino; this was done so that it moved enough for the attached tubing to reach the bottom of each well, and then also to raise enough so that the tubing would not drag along other wells when the plate moved in the x- and y- direction. Hypodermic tubing was then secured to the slide pot so that the rigid plastic tubing would be secured to it simply by sliding it in, allowing for easy switching of tubing.

7.4 Experimental Methods

7.4.1 Overview

Once the system's ability to move in the x-, y-, and z- directions, to elicit chemical flow, was confirmed, the system needed validation testing to ensure that the efficacy of the system was on par with the manual method. Cross-contamination rate from one well to the next was investigated by using fluorescein. Once the cross-contamination rate was at the accepted amount of less than 0.01%, the system's viability was confirmed with live animal testing that could be compared to existing data.

7.4.2 Fluorescein Cross-contamination Testing

Cross-contamination is a serious concern when screening drugs; without the ability to distinguish individual drugs from one another, the response data will be corrupted. Therefore, we had the goal of achieving a chemical cross-contamination of less than 0.01% between drug switches. To quantify the cross-contamination of the system, the team used fluorescein to measure the cross-contamination between trials. Two methods were used to test cross-

contamination rate. In one method, fluorescein was sequentially tested with DI-water, and the amount of fluorescence that carried over from the previous fluorescein well into the successive DI-water well, after subtracting the baseline of fluorescence of the PDMS, indicated the cross-contamination. A second method, which included a DI-water rinse after each chemical switch, was then used to see if the resulting cross-contamination would be reduced due to a rinse.

7.4.3 Live Animal Testing

To confirm the efficacy of our system further, we conducted live animal testing using *C. elegans*. We replicated a study previously conducted by Larsch et al., where the AWA neurons respond to diacetyl exposure. The team's automated dose response was conducted at six different concentrations of diacetyl (0.1 µM, 1 µM, 10 µM, 100 µM, 1,000 µM, and 10,000 µM) with three pulses each on 11 animals, and the animals' neural responses were analyzed. The highest two concentrations (i.e. 1,000 µM and 10,000 µM) were omitted from our comparison to previous studies, due in part to the lack of existing data for these particular concentrations. After speaking with our advisor, we deduced that the differences in the results for these two concentration levels could be due to saturation of neural responses, as well as adaptation of the animals to the chemical stimulus.

7.4.4 Experimental Setup

We conducted these experiments in a similar fashion to that described in Section 4.6.4, with the exception that all four of the device's inlets were punched, allowing us to deliver chemical pulses.

7.5 Results

From the fluorescein study, we found that the inclusion of a rinse cycle between chemical switches effected a cross-contamination between chemicals that was within our initial cross-contamination constraint of 0.01%. The cross-contamination rate with no rinse was found to be 0.025% while including a rinse reduced the cross-contamination to 0.0074%, meeting our constraint of being lower than 0.01%. A complete chemical switch between well A1 to well A2 occurred within approximately 50 seconds, which was also within our switching speed constraint of 60 seconds.

Building off of our previous successful results, we conducted animal studies evaluating the AWA neural response of *C. elegans* when exposed to different concentrations of diacetyl. Our system was effective in eliciting the expected *C. elegans* neural responses, after we replicated a portion of the previously mentioned Larsch et al. Study. Our results, represented in Figure 38, show the fluorescent response of the nematodes' AWA neurons increasing with higher concentrations of diacetyl. This matches the results found by Larsch et al. with minimal differences. Lastly, our entire project had a budget of $500 to create the automated system. We only ended up spending $252.31 for everything we used, so we managed our budget very well by choosing good components at an ideal price. It is worth noting that the entire set up could not be replicated for this amount, due to the cost of the camera, but the automated system component that we constructed was able to fit within all of our restrictions.

Chapter 8: Conclusions and Recommendations

As discussed in Chapter 6, the potential impact of our system is immense. Because our system is able to accurately replicate a neural chemical screening experiment conducted manually using *C. elegans*, the effects of the Larsch et al. study are intertwined with the effects of the creation of our system. Additionally, our system has the added effect of increasing the throughput of screening experiments that were already high-throughput to begin with. The implications of neural screening experiments in general, associated with the increased throughput of such experiments, essentially entails that our system can indirectly improve the quality of life of millions of people worldwide who suffer from neuropsychiatric illness, at a faster pace than current research methods. Moreover, the researcher can spend the 242 hours it takes to test all of the pharmacologically active compounds available completing other research or tasks, thus increasing the individual researcher's overall productivity, which in turn can increase the overall productivity of all researchers worldwide.

Before going ahead and testing all 1,280 chemicals, we recommend testing the system even more to see that it is reliable and consistent. While we tested the flow rate and the cross-contamination for the switching of chemicals, there was more that could have been done to make sure the system would be able to handle so hundreds of hours of work. The maximum number of wells we tested using the automated system was 12, which was performed in both the cross-contamination and the *C. elegans* automated dose response studies. The system did not run into any problems when it came to this, but to ensure ideal performance, we recommend running several tests where all 96 wells of the plate are accessed. This should be done several times, timing each trial to make sure the timing is consistent as well. Another reliability factor we could test is the depth the tubing travels in each well. This could be done by filling all of the wells with

a certain amount of liquid and then timing each one until the well is empty. If the wells do not drain at the same rate, then the thresholds for dipping into the wells would need to be changed. One more reliability aspect that can be challenged, which would be lengthy, is to test how many Press N' Seal wrap punctures the sharp tubing can endure before becoming dull. This could be done by just having the system rapidly puncture different well covers until the tubing fails to puncture on the first try. This would give an estimate as to how often the tubing needs to be cut to ensure proper function.

Although we were able to reach the goals we had for our system, there are several improvements that can be made to our system, thus strengthening the positive impact it has even further. One potential improvement is crafting the plate holder platform out of aluminum. This is desirable because the durability of aluminum is much greater than that of 3-D printed plastic and is light enough to not impact how the system functions. Another potential improvement is creating a remote video monitoring system that the experimenter could check from their office, home, or even on their smartphone. By allowing for viewing of the system remotely, the experimenter can ensure that the experiment is running properly and safely, as any unattended use of chemicals should be handled carefully. A major potential improvement to our system would be the ability for it to self-diagnose and solve errors that have occurred. By implementing measures to ensure consistent flow rate and proper imaging, time and materials could be saved so that no trial is wasted due to an error occurring. One last improvement that could be made is to make the overall system safer. While the system is currently only available to trained personnel that have specifically been given access, there is a need to ensure that chemical spills do not interact with electronics or humans in the area. A constantly running vacuum system where potential leaks may occur would ensure that chemicals are not displaced in an undesired area.

Additionally, some kind of protective shielding could be useful to limit the exposure the chemicals have with humans if there were to be a spill.

References

1. "Academic Screening Facilities." *SLAS*. Society for Laboratory Automation and Screening. Web. 14 Apr. 2015.
2. "Adafruit Motor Shield V2 for Arduino." *Adafruit*. 9 July 2013. Web. 26 Sept. 2014. <https://learn.adafruit.com/adafruit-motor-shield-v2-for-arduino>."Arduino - Introduction." *Arduino*. Web. 26 Sept. 2014. <http://arduino.cc/en/Guide/Introduction>.
3. Ankeny, Rachel A. "The natural history of Caenorhabditis elegans research." *Nature Reviews Genetics* 2.6 (2001): 474-479.
4. "Arduino Uno." *Arduino*. Web. 26 Sept. 2014. <http://arduino.cc/en/Main/ArduinoBoardUno>.
5. "Autism Fact Sheet." *National Institute of Neurological Disorders and Stroke (NINDS)*. National Institute of Neurological Disorders and Stroke, Sept. 2009. Web. 26 Sept. 2014.
6. "Autism Main Symptoms." *Evening Chronicle* 7 Aug. 2006, 1st ed., NEWS sec.: 4. Print.
7. Azevedo et al. "Equal numbers of neuronal and nonneuronal cells make the human brain an isometrically scaled-up primate brain." *Journal of Comparative Neurology*, 513.5, pp. 532-41, 2009.
8. B.S. Abrahams and D.H. Geschwind. "Advances in autism genetics: on the threshold of a new neurobiology." *Nature Reviews Genetics*, 9.5, pp. 341-55, 2008.
9. Baio, Jon. "Prevalence of Autism Spectrum Disorders: Autism and Developmental Disabilities Monitoring Network, 14 Sites, United States, 2008. Morbidity and Mortality Weekly Report. Surveillance Summaries. Volume 61, Number 3." *Centers for Disease Control and Prevention* (2012).
10. Bear, Mark F., Barry W. Connors, and Michael A. Paradiso, eds. *Neuroscience*. Vol. 2. Lippincott Williams & Wilkins, 2007.
11. Blum, Jeremy. Exploring Arduino: Tools and Techniques for Engineering Wizardry. Somerset, NJ, USA: John Wiley & Sons, 2013. ProQuest ebrary. Web. 16 October 2014.
12. Bono, Mario de, and Andres Villu Maricq. "Neuronal substrates of complex behaviors in *C. elegans*." *Annu. Rev. Neurosci.* 28 (2005): 451-501.
13. Boyd, Windy A., Sandra J. McBride, and Jonathan H. Freedman. "Effects of genetic mutations and chemical exposures on Caenorhabditis elegans feeding: evaluation of a novel, high-throughput screening assay." *PLoS One* 2.12 (2007): e1259.
14. Brenner, Sydney. "The genetics of Caenorhabditis elegans." *Genetics* 77.1 (1974): 71-94.
15. Calahorro F. and Ruiz-Rubio M. "Caenorhabditis elegans as an experimental tool for the study of complex neurological diseases: Parkinson's disease, Alzheimer's disease and autism spectrum disorder." *Invertebrate neuroscience*, 11.2, pp. 73-83, 2011.
16. Caldwell, G. A. and Caldwell, K. A. "Traversing a wormhole to combat Parkinson's disease." *Disease models & mechanisms* 1.1, pp. 32-6, 2008.
17. Chalfie, Martin, and Erik M. Jorgensen. "*C. elegans* neuroscience: genetics to genome." *Trends in Genetics* 14.12 (1998): 506-512.
18. Chesselet M. F., and Carmichael S. T. "Animal models of neurological disorders." *Neurotherapeutics*, pp. 1-4, 2012.
19. *Copas* [Online]. Available: http://www.unionbio.com/copas/
20. Cupido, Paul N., Yu Feng, and Justin P. Hess. *NeuroTracker 2.0: Improved Software for Neural Imaging in Freely-Moving Animals*. Ed. Dirk Albrecht, Joseph B. Duffy, and

Matthew O. Ward. *Electronic Projects Collection*. Worcester Polytechnic Institute, 1 May 2014. Web. 5 Oct. 2014.
21. Dickinson, Daniel J., et al. "Engineering the Caenorhabditis elegans genome using Cas9-triggered homologous recombination." *Nature methods* 10.10 (2013): 1028-1034.
22. Erhart, Stephen M., Stephen R. Marder, and William T. Carpenter. "Treatment of schizophrenia negative symptoms: future prospects." *Schizophrenia Bulletin* 32.2 (2006): 234-237.
23. Félix, Marie-Anne, and Christian Braendle. "The natural history of Caenorhabditis elegans." *Current Biology* 20.22 (2010): R965-R969.
24. Fombonne, E. "The Prevalence of Autism." *JAMA: The Journal of the American Medical Association* 289.1 (2003): 87. Print.
25. Giacomotto et al. "Caenorhabditis elegans as a chemical screening tool for the study of neuromuscular disorders. Manual and semi-automated methods." *Methods,* 56, 1, pp. 103-13, 2012.
26. Gilbert SF. Developmental Biology. 10th edition. Sunderland (MA): Sinauer Associates; 2013.
27. Goode, David J., and Alexander A. Manning. "Specific imbalance of right and left sided motor neuron excitability in schizophrenia." *Journal of Neurology, Neurosurgery & Psychiatry* 51.5 (1988): 626-629.
28. Gosai, Sager J., et al. "Automated high-content live animal drug screening using *C. elegans* expressing the aggregation prone serpin α1-antitrypsin Z." *PloS one* 5.11 (2010): e15460.
29. Greene, J. and Griffin, C. (2007, September 4) "BioTek Instruments, Inc. Unveils MicroFlo™ Select with Unlimited Liquid Dispensing Flexibility." *BioTek.* [Online] Available: http://www.biotek.com/about/news.html?id=8695
30. Hope, Ian A. *C. elegans: a practical approach*. Oxford University Press (OUP), 1999.
31. Houltram, Brian, and Mike Scanlan. "Extrapyramidal side effects." *Nursing Standard* 18.43 (2004): 39+. *Academic OneFile*. Web. 16 Oct. 2014.
32. Hyman, Steven E., and Eric J. Nestler. "Animal models of neuropsychiatric disorders." *Nature Neuroscience* 13.10 (2010): 1161+. *Health Reference Center Academic*. Web. 15 Oct. 2014.
33. "Introduction to *C. elegans*." *Wormatlas.* 2006. Web. 12 Oct. 2014
34. Jahromi, Laudan B., et al. "Positive effects of methylphenidate on social communication and self-regulation in children with pervasive developmental disorders and hyperactivity." *Journal of autism and developmental disorders* 39.3 (2009): 395-404.
35. Jones, Andrew K., Steven D. Buckingham, and David B. Sattelle. "Chemistry-to-gene screens in Caenorhabditis elegans." *Nature Reviews Drug Discovery* 4.4 (2005): 321-330.
36. L298 Dual Full Bridge Driver. (n.d.). Retrieved March 5, 2015, from http://www.st.com/web/en/catalog/sense_power/FM142/CL851/SC1790/SS1555/PF63147
37. Lai, Meng-Chuan, Michael V Lombardo, and Simon Baron-Cohen. "Autism." *The Lancet* 383.9920 (2014): 896-910. Print.
38. Lai, Chun-Hung, et al. "Identification of novel human genes evolutionarily conserved in Caenorhabditis elegans by comparative proteomics." Genome research 10.5 (2000): 703-713.

39. Larsch, Johannes, et al. "High-throughput imaging of neuronal activity in Caenorhabditis elegans." *Proceedings of the National Academy of Sciences*110.45 (2013): E4266-E4273.
40. Larson, Brad, et al. "Automation of Cell-Based Drug Absorption Assays in 96-Well Format Using Permeable Support Systems." *Journal of laboratory automation* 17.3 (2012): 222-232.
41. Leucht, Stefan, et al. "Comparative Efficacy and Tolerability of 15 Antipsychotic Drugs in Schizophrenia: A Multiple-treatments Meta-analysis." *The Lancet* 382.9896 (2013): 951-62. Print.
42. Leucht, S, et al. "Maintenance Treatment with Antipsychotic Drugs for Schizophrenia." *COCHRANE DATABASE OF SYSTEMATIC REVIEWS*.5 (2012) Web. 16 Oct. 2014.
43. Leung, Maxwell CK, et al. "Caenorhabditis elegans: an emerging model in biomedical and environmental toxicology." *Toxicological Sciences* 106.1 (2008): 5-28.
44. Levy, Susan, David Mandell, and Robert Schultz. "Autism." *The Lancet* 374.9701 (2011): 1627-638. Print.
45. Liu, Leo X., et al. "High-throughput isolation of Caenorhabditis elegans deletion mutants." *Genome research* 9.9 (1999): 859-867.
46. Macarron, Ricardo, et al. "Impact of high-throughput screening in biomedical research." *Nature reviews Drug discovery* 10.3 (2011): 188-195.
47. "MakerSlide: Open Source Aluminum Extrusion with V-rail Linear Bearing System Built in." *Inventables*. Web. 26 Apr. 2015.
48. Marder, Stephen R., et al. "Aripiprazole in the treatment of schizophrenia: safety and tolerability in short-term, placebo-controlled trials." *Schizophrenia research* 61.2 (2003): 123-136.
49. Matson, Johnny L., and Julie A. Hess. "Psychotropic drug efficacy and side effects for persons with autism spectrum disorders." *Research in Autism Spectrum Disorders* 5.1 (2011): 230-236.
50. McGrath, J., S. Saha, D. Chant, and J. Welham. "Schizophrenia: A Concise Overview Of Incidence, Prevalence, And Mortality." *Epidemiologic Reviews* 30.1 (2008): 67-76. Print.
51. McRoberts, Michael. "What Exactly Is an Arduino?" *Beginning Arduino*. Second ed. Apress, 2013. Print.
52. Odle, Teresa G., Donald G. Barstow, and Laura Jean Cataldo. "Pervasive Developmental Disorders." *The Gale Encyclopedia of Medicine*. Ed. Laurie J. Fundukian. 4th ed. Vol. 5. Detroit: Gale, 2011. 3361-3364. *Gale Virtual Reference Library*. Web. 16 Oct. 2014.
53. O'Reilly, Linda P., et al. "*C. elegans* in high-throughput drug discovery." *Advanced drug delivery reviews* 69 (2014): 247-253.
54. Parce, J. Wallace, Anne R. Kopf-Sill, and Luc J. Bousse. "High throughput screening assay systems in microscale fluidic devices." U.S. Patent No. 6,267,858. 31 Jul. 2001.
55. Parelkar, Sangram. "Small Molecule Screening Facility (SMSF)." *University of Massachusetts Medical School*. Web. 18 Apr. 2015.
56. Phillips, Carolyn M., and Abby F. Dernburg. "A Family of Zinc-Finger Proteins Is Required for Chromosome-Specific Pairing and Synapsis during Meiosis in *C. elegans*." *Developmental cell* 11.6 (2006): 817-829.
57. Parker et al. "Antipsychotic drugs and risk of venous thromboembolism: nested case-control study." *The BMJ*, 341:c4245, 2010.
58. *Pipetmax* [Online]. Available: http://www.gilson.com/en/AI/Products/13.290/Default.aspx

59. Purves D, Augustine GJ, Fitzpatrick D, et al., editors. Neuroscience. 2nd edition. Sunderland (MA): Sinauer Associates; 2001. Two Major Categories of Neurotransmitters. Available from: http://www.ncbi.nlm.nih.gov/books/NBK10960/
60. Riddle, Donald, Thomas Blumenthal, Barbara Meyer, and James Priess, eds. "*C. elegans* II, 2nd Edition." *Cold Spring Harbor Monograph Series* 33 (1997). Print.
61. Riddle D. (1988). In "The nematode *C. elegans*" (W. B. Wood ed.) pp393-412. Cold Spring Harbor Laboratory Press, New York
62. San-Miguel, Adriana, and Hang Lu. "Microfluidics as a tool for *C. elegans* research." (2005).
63. Santosh, Paramala Janardhanan, and Gillian Baird. "Pharmacotherapy of target symptoms in autistic spectrum disorders." *The Indian Journal of Pediatrics* 68.5 (2001): 427-431.
64. Schneider, Caroline A., et al. " NIH Image to ImageJ: 25 years of image analysis" *Nature methods* 9.7 (2012): 671-675.
65. "Shields/3rd Party." *Arduino*. Web. 16 Oct. 2014. <http://store.arduino.cc/category/38>.
66. Sin, Olga, Helen Michels, and Ellen AA Nollen. "Genetic screens in Caenorhabditis elegans models for neurodegenerative diseases."*Biochimica et Biophysica Acta (BBA)-Molecular Basis of Disease* (2014).
67. Sleigh J. N., and Sattelle D. B. "*C. elegans* models of neuromuscular diseases expedite translational research." *Translational Neuroscience* 1.3 pp. 214-27, 2010.
68. Squire, Larry R., ed. *Fundamental neuroscience*. Academic Press, 2008.
69. "Standard Wheel Carriage Plate: General Purpose Carriage Plate for MakerSlide Linear Rail." *Inventables*. Web. 26 Apr. 2015.
70. Sulston, J. E., D. G. Albertson, and J. N. Thomson. "The Caenorhabditis Elegans Male: Postembryonic Development of Nongonadal Structures." *Developmental Biology* 78.2 (1980): 542-76. Print.
71. White J. (1988). In "The nematode *C. elegans*" (W. B. Wood ed.) pp81-122. Cold Spring Harbor Laboratory Press, New York.
72. "Wireless SD Shield." *Arduino*. Web. 26 Sept. 2014. <http://arduino.cc/en/Main/ArduinoWirelessShield>.
73. Wood, William Barry. *The nematode Caenorhabditis elegans*. Cold Spring Harbour Laboratory, 1987.

Appendix A

```
int val = 0;
int DirA = 12;
int PWMA = 3;
int BrakeA = 9;
int i = 0;
void setup()
{
    Serial.begin(9600);
    pinMode(DirA, OUTPUT);
    pinMode(PWMA, OUTPUT);
    pinMode(BrakeA, OUTPUT);
}

void loop()
{
    val = analogRead(3);
    Serial.println(val);

/*
digitalWrite(DirA, HIGH);
analogWrite(PWMA, 255);
delay(250);
digitalWrite(DirA, HIGH);
analogWrite(PWMA, 0);
delay(500);
digitalWrite(DirA, LOW);
analogWrite(PWMA, 255);
delay(500);
digitalWrite(DirA, LOW);
analogWrite(PWMA, 0);
delay(30000);
*/
// Starts at motor
while(i<5){
        down(); // Goes down at max speed
        stop(3); // Stops at bottom of slide pot for 3 seconds
        up();
        stop(1); // Stops near motor for 1 second
        down();
        stop(0.5); // Stops at bottom for half a second
        up();
        stop(1); // Stops near motor again for 1 second
        i++; // Goes through 5 iterations of entire loop
    }
}


void down(){ // Describes down command
    digitalWrite(DirA, HIGH); // Knob travels in Direction A (away from start)
    analogWrite(PWMA, 255); // Details speed of knob motion (max speed)
    delay(500);
}

void up(){
    digitalWrite(DirA, LOW);
    analogWrite(PWMA, 255);
    delay(500);
}

void stop(int value){
    digitalWrite(DirA,LOW);
    analogWrite(PWMA,0);
    delay(value *1000);
}
```

Appendix B

```
//  MQP Slide Pot Controls
//  This program controls the Z-axis movement of the automated system.

int val = 0;
int DirA = 12;
int PWMA = 3;
int BrakeA = 9;
int i = 0;
void setup()

{
    Serial.begin(9600);
    pinMode(DirA, OUTPUT);
    pinMode(PWMA, OUTPUT);
    pinMode(BrakeA, OUTPUT);
    origin();
}


void loop()
{
    origin();       //  Moves from last current position to the origin

    while(i<5){
        origin();   //  Moves to the origin
        down(1);    //  Moves down at max speed for 1 second
        stop(3);    //  Stops at bottom of slide pot for 3 seconds
        origin();   //  Moves up to origin
        stop(1);    //  Stops at origin for 1 second
        down(1);    //  Moves down for 1 second
        stop(1);    //  Stops at bottom for 0.5 seconds
        origin();   //  Moves up to origin
        stop(1);    //  Stops at origin for 1 second
        i++;        //  Goes through the loop with "i" number of interations
    }
}

void origin(){      //  Homes slide to origin around 377
    int desiredVal = 400;
    val = analogRead(3);
    while(val>450 || val<350){
        val = analogRead(3);
        Serial.println(val);
        int delta = desiredVal - val;
        if((delta > 0)&&(val<350)){
            up(0.01);}
        else if((delta < 0)&&(val>450)){
            down(0.01);}
        else stop(0.01);}
}

void down(int value){           //  Down movement function
    digitalWrite(DirA, HIGH);   //  Moves in Direction A (away from start)
    analogWrite(PWMA, 255);     //  Details speed of motion (max speed)
    delay(value *1000);
}

void up(int value){             //  Up movement function
    digitalWrite(DirA, LOW);
    analogWrite(PWMA, 255);
    delay(value *1000);
}

void stop(int value){           //  Stop movement function
    digitalWrite(DirA,LOW);
    analogWrite(PWMA,0);
    delay(value *1000);
}
```

Appendix C

```
/*
For use with the Adafruit Motor Shield v2
---->   http://www.adafruit.com/products/1438
*/

#include <Wire.h>
#include <Adafruit_MotorShield.h>
#include "utility/Adafruit_PWMServoDriver.h"
//#include <Servo.h>

// Create the motor shield object with the default I2C address
Adafruit_MotorShield AFMS = Adafruit_MotorShield();

// Connect a stepper motor with 200 steps per revolution (1.8 degree)
Adafruit_StepperMotor *xMotor = AFMS.getStepper(200, 1);
Adafruit_StepperMotor *yMotor = AFMS.getStepper(200, 2);

//Servo zServo;

const int stepSize = 45;
// 20 tooth gear --> 0.2 mm/step, 9 mm well-to-well spacing on 96-well plate
const int upZpos = 1000;
const int downZpos = 2000;

const int xMinLimitPin = 4;
const int xMaxLimitPin = 5;
const int yMinLimitPin = 6;
const int yMaxLimitPin = 7;

const int DirA = 12;
const int PWMA = 3;
const int BrakeA = 9;
const int zPosPin = 3;

int i = 0;
int val = 0;

const boolean showStatus = false; // print status info to serial port

boolean limitReached;
int limitState = 0;
int priorState = 0;
int ypos = 0;
int xpos = 0;
int newypos = 0;
int newxpos = 0;
int dy = 0;
int dx = 0;
int A1x = 32; // x-steps from home to A1 well position
int A1y = 31; // y-steps from home to A1 well position

void setup()
{
    Serial.begin(9600);           // set up Serial library at 9600 bps

    AFMS.begin();  // create with the default frequency 1.6KHz

    xMotor->setSpeed(200);  // rpm
    yMotor->setSpeed(200);  // rpm

    //zServo.attach(10);

    pinMode(xMinLimitPin, INPUT_PULLUP);
    pinMode(xMaxLimitPin, INPUT_PULLUP);
    pinMode(yMinLimitPin, INPUT_PULLUP);
    pinMode(yMaxLimitPin, INPUT_PULLUP);

    pinMode(DirA, OUTPUT);
```

```
    pinMode(PWMA, OUTPUT);
    pinMode(BrakeA, OUTPUT);
}

void loop()
{

    while (Serial.available() > 0)
    {

        char row = Serial.read();  // read row character A...H
        int col = Serial.parseInt(); // read column integer 1 - 12
        char z = Serial.read(); // read z-position "+"=up, "-"=down
        int rem = Serial.parseInt();

        newypos = row - 'A' + 1;
        newxpos = col;

        //zServo.writeMicroseconds(upZpos);
        setZpos(500); // move to up position
        delay(100);

        if (newypos == -16)    // '0' to home and move to well A1
        {

            // home the stage
            homeStage();

            // Adjust to well A1 position
            limitReached = MoveStepsAndCheckLimits(A1x, A1y);
            if (limitReached && showStatus)
            {
                Serial.println("Warning!! Limit Reached");
            }

            ypos = 1;
            xpos = 1;
            z = '+';   // home with z-position up

        }
        else
        {

            // handle y-position
            if (newypos < 1) newypos = ypos;
            if (newypos > 8) newypos = ypos;
            dy = newypos - ypos;

            // handle x-position
            if (newxpos < 1) newxpos = xpos;
            if (newxpos > 12) newxpos = xpos;
            dx = newxpos - xpos;

            // move steppers
            limitReached = MoveStepsAndCheckLimits(dx * stepSize, dy * stepSize);

            if (limitReached && showStatus)
            {
                Serial.println("Warning!! Limit Reached");
            }

            // Update positions
            ypos = newypos;
            xpos = newxpos;
        }

        // Release power to motors
        xMotor->release();
```

```
        yMotor->release();

        // Handle z-position
        delay(300);
        if (z == '+')
        {
            //zServo.writeMicroseconds(upZpos);
            setZpos(500);
            Serial.print(z);
        }
        else if (z == '-')
        {
            //zServo.writeMicroseconds(downZpos);
            setZpos(70);
            Serial.print(z);
        }

        delay(300);
        // Send serial command to confirm new position and motor completion
        Serial.print(row);
        Serial.print(col);
        Serial.println(z);
        Serial.println("OK");


    }

    if (showStatus)
    {
        priorState = limitState;
        limitState = readLimitSwitches();
        if (limitState != priorState) Serial.println(limitState);
        delay(50);
    }

}

void homeStage()
{
    // home y-axis
    boolean yHome = false;
    while (!yHome)
    {
        yHome = MoveStepsAndCheckLimits(0, -1);
    }
    if (showStatus) Serial.println("Home on y-axis");

    delay(100);

    // home x-axis
    boolean xHome = false;
    while (!xHome)
    {
        xHome = MoveStepsAndCheckLimits(-1, 0);
    }
    if (showStatus) Serial.println("Home on x-axis");
}

int readLimitSwitches()
{
    int limitState  = !digitalRead(xMinLimitPin) * 8;
    limitState += !digitalRead(xMaxLimitPin) * 4;
    limitState += !digitalRead(yMinLimitPin) * 2;
    limitState += !digitalRead(yMaxLimitPin) * 1;

    return limitState;
}

```

```
boolean MoveStepsAndCheckLimits(int stepx, int stepy)
{

    //boolean limitReached = false;
    boolean xfwd = (stepx < 0);
    boolean yfwd = (stepy > 0);

    int limitState = readLimitSwitches();
    boolean limitReached = (limitState > 0);

    stepx = abs(stepx);
    stepy = abs(stepy);

    while (((stepx > 0) || (stepy > 0)) && !limitReached)
    {

        if (stepx > 0)
        {
            if (xfwd)
            {
                xMotor->onestep(FORWARD, DOUBLE);
            }
            else
            {
                xMotor->onestep(BACKWARD, DOUBLE);
            }
            stepx--;
        }

        if (stepy > 0)
        {
            if (yfwd)
            {
                yMotor->onestep(FORWARD, DOUBLE);
            }
            else
            {
                yMotor->onestep(BACKWARD, DOUBLE);
            }
            stepy--;
        }

        limitState = readLimitSwitches();
        limitReached = (limitState > 0);
    }

    // delay(10);
    // Handle Limits: back off
    while ((limitState & B1000) > 0)
    {
        xMotor->onestep(FORWARD, DOUBLE);
        limitState = readLimitSwitches();
    }
    while ((limitState & B0100) > 0)
    {
        xMotor->onestep(BACKWARD, DOUBLE);
        limitState = readLimitSwitches();
    }
    while ((limitState & B0010) > 0)
    {
        yMotor->onestep(FORWARD, DOUBLE);
        limitState = readLimitSwitches();
    }
    while ((limitState & B0001) > 0)
    {
        yMotor->onestep(BACKWARD, DOUBLE);
        limitState = readLimitSwitches();
    }
```

```
273
274     /*
275     if ((limitState & B1000) > 0) xMotor->onestep(FORWARD, DOUBLE);
276     if ((limitState & B0100) > 0) xMotor->onestep(BACKWARD, DOUBLE);
277     if ((limitState & B0010) > 0) yMotor->onestep(FORWARD, DOUBLE);
278     if ((limitState & B0001) > 0) yMotor->onestep(BACKWARD, DOUBLE);
279     */
280
281     return limitReached;
282 }
283
284 void setZpos(int zPosition){
285
286     int moveComplete = false;
287
288     while (moveComplete == false) {
289
290         val = analogRead(zPosPin);   // get current position
291         int delta = zPosition - val;
292         Serial.print(val); Serial.print("  "); Serial.println(delta);
293
294         if (abs(delta) < 20) {
295             analogWrite(PWMA,0);    // stop motor
296             moveComplete = true;
297         } else {
298             if (delta > 0) digitalWrite(DirA, LOW);
299             else digitalWrite(DirA, HIGH);
300             analogWrite(PWMA, max(100,min(170,abs(delta))));
301         }
302     }
303 }
304
```

Appendix D

The following schematic displays the dimensions of the 96-well plate platform that we used in our automated system.